VOLUME 3, NUMBER 1

Geotechnical Journal

JANUARY 2006

Sri Lankan Geotechnical Society

Geotechnical Journal

Sri Lankan Geotechnical Society
C/o National Building Research Organisation
99/1, Jawatta Road, Colombo 5,
Sri Lanka

EDITED BY :

Dr. U.G.A. Puswewala

ARTICLES REVIEWED BY :

Prof. B.L. Tennekoon
Prof. H.N. Seneviratna
Prof. M. Gunaratne
Prof. K.A.M.K. Ranasinghe
Prof. V.B.N. Indraratne

Hazard and Risk Assessment in Landslide Prone Hill Country of Sri Lanka

ABEYSINGHE[1, 2], A.M.K.B., IWAO[1], Y., SAITO[1], A and BANDARA[2], R.M.S

[1] Department of Civil Engineering, Graduate School of Science and Engineering, Saga University, Japan
[2] Landslide Studies & Services Division, National Building Research Organisation, 99/1, Jawatte Road., Colombo 5, Sri Lanka

ABSTRACT : The hill country of Sri Lanka, underlain by highly folded and fractured metamorphic rocks of different grades of weathering have a high probability for landslides and rock-falls. Intense precipitation is a major factor contributing to the landslides. Despite repeated occurrences of landslides in Sri Lanka inflicting losses in terms of life and property, very little has been done towards introducing scientific practices for delineating the degrees of hazard, identifying elements at risk, and landslide risk assessment. National Building Research Organization (NBRO) has already commenced production of landslide hazard zonation maps covering the areas prone to landslides. Those maps and data are expected to provide an essential input to the risk assessment. The present study was based on an investigation carried out in Yatiyantota area at Kegalle district. The area was severely affected by the landslide incidents that occurred in 1997 during the north - west monsoons. Development of a culture for, assessment of risk before commencement of major infrastructure development projects and establishment of human settlements in landslide prone areas based on the risk criterion will be essential for sustainable development of the central hills of Sri Lanka.

Keywords: Landslides, Hazard mapping, Risk assessment, Elements at risk, Vulnerability.

1.0 Introduction

1.1 General

Landslides are a common natural phenomenon in many parts of the world, especially in hilly or mountainous terrains. A landslide event is defined as "the movement of a mass of rock, debris, or earth (soil) down a slope (under the influence of gravity). The word "landslide" also refers to the geomorphic feature that results from the event. Other terms used to refer to landslide events include; mass movements, slope failures, slope instability and terrain instability.

In Sri Lanka during the last few decades, landslides occurred with increasing frequency in the hill country. The hill country, underlain by highly folded, fractured and weathered metamorphic rocks, has a high probability for landslides.

Intense precipitation is a major factor contributing to the occurrence of landslides. The above mentioned area covers an approximate extent of 10,000 sq.km. It is about 20% of the total area of the island and occupied by about 30% of the total population of Sri Lanka. Seven administrative districts within the hill country are prone to landslides, namely, Badulla, Nuwara Eliya, Rathnapura, Kegalle, Kandy, Matale and Kalutara. In the recent memory, peaks of landslide disasters had occurred in January 1986, May/ June 1989, October 1993, September 1997and April/ May 2002. Disasters due to landslide hazards have brought significant economic and social impact causing severe damages to life and property, the environment, and socio-economic life of the society.

This paper highlights the on-going landslide hazard zonation mapping programme and a newly developed method for landslide risk assessment in the hill country of Sri Lanka.

1.2 Geology, Geomorphpology and Rainfall of Hill Country

The area in the central highlands is mainly covered by Precambrian metamorphic rocks belonging to the Highland Complex (Cooray, 1978). This series consist of quartzite, garnet silimanite gneiss, marble, and charnockitic gneiss.

All these rocks have been expected to be deformed under conditions of granulite facies into open, tight, upright and overturned antiforms and synforms (Berger and Jayasinghe 1976). The central hilly areas of Sri Lanka has been categorized as uplands and highlands by Vitanage (1985). Elevation of the hill ranges varies from about 180m to 2717m MASL, of which the highest is at the Piduruthalagala peak (Figure 1). Normally ridges and valleys characterize the general morphology of the areas with high relief. As a general factor, most of the hill slopes are covered with thick overburden deposits, mostly colluviums and lateritic residual soils.

During the last two decades, landslide incidents have been observed with increasing frequency in the hilly areas. Landslides are very often triggered by continuous rainfall characterized by showers of high intensity that occur for short periods of time. Central highlands of Sri Lanka experiences rain from two monsoons, North-East and South-West. Annual average rainfall in the area varies from 5500mm in the South-West and mid country to 1750mm in the North-East.

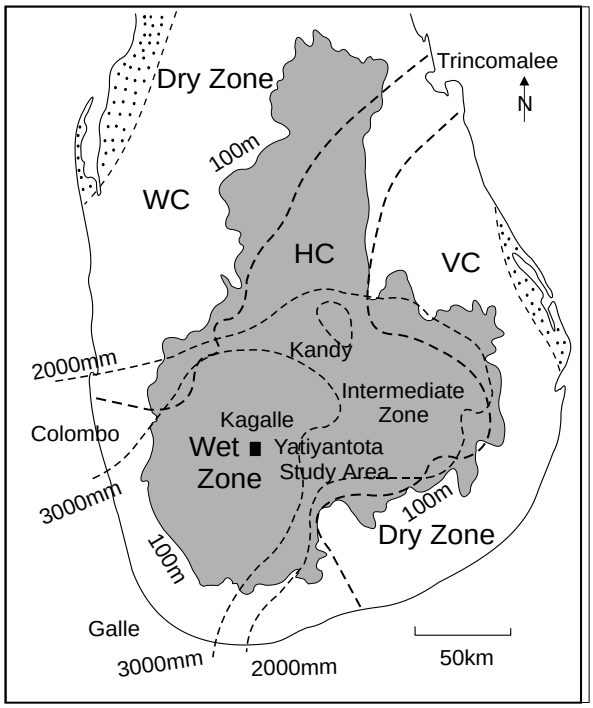

Figure 1 : Sketch Map of Sri Lanka Showing
(a) land over 180m
(b) wet zone over 3000mm annual rainfall, intermediate zone (2000-3000mm) and dry zone less than 2000mm.
(c) main lithological units
HC- Highland Group, WC- Wanni Complex, VC- Vijayan Complex, dotted sedimentary rocks.

A significant feature of some recent landslides in the hill country is the reactivation of dormant ancient slides that were in equilibrium state for a considerable time. The reactivation may be due to natural reasons or man's interference.

1.3 Landslide Risk Management of Hill Country of Sri Lanka

Landslide risk management, like many other forms of risk management of natural and/or civil engineering hazards, is a relatively new discipline with evolving analytical techniques. Risk management is relatively well established in other industries, particularly in the nuclear and hazardous processing industries, where standards for risk analysis and risk management have been developed. Recent advances in risk management for slopes and landslides are beginning to provide systematic and rigorous processes to formalize the engineering judgments and enhance slope-engineering practices. The risk management process comprises three components, namely, risk analysis, risk evaluation and risk treatment. Risk analysis and risk evaluation are sub-sets of risk assessment and risk assessment and risk treatment are sub-sets of risk management. In simple form, the process involves answering the following questions;

- What might happen? Landslide hazard identification.
- How often is it? Frequency of occurrence of failure.
- What damage or injury may result? Consequences of failure.
- How important is it? Acceptability of landslide risk.
- What can be done about it? Landslide risk treatment.

Procedures for landslide risk management including risk assessment have not been standardized in the past, although use of "risk" or "hazard" zoning maps is widespread internationally. The papers by Varnes (1984), Whitman (1984), Einstein (1988), Morgan et. all (1992), Fell (1994), Einstein (1997) Fell and Hartford (1997) and Australian Geomechanics Society (2000), give overviews of this subject.

Qualitative landslide risk assessment involves acquiring knowledge of the hazards, the elements at risk and their vulnerabilities, and expressing that knowledge qualitatively, typically as ranked attributes or expressed verbally. The risk may then be expressed verbally or ranked. With more sophisticated assessments, there is an increasing use of quantitative expression of the input parameters which then contributes to a form of quantitative risk assessment.

The 1986/89 major landslide disasters prompted the Government of Sri Lanka to take serious note of the losses and initiate appropriate measures for reduction of the impact of landslide disasters. As a result, the National Building Research Organization (NBRO), attached to the Ministry of Housing and Plantation Infrastructure, was selected as an appropriate multi-disciplinary organization for building the institutional capacity in the field of landslide studies and services under Landslide Hazard Mapping Program (LHMP) started in 1990. This program received financial and technical support from the United Nations Development Programme (UNDP) and United Nations Center for Human Settlements (UNCHS) at the initial stage of the program. From the seven landslide prone districts, Badulla and Nuwara Eliya were the worst affected and therefore were selected for initiation of landslide hazard mapping work (Phase I). Although the phase I of the program ended in July 1995, the Government of Sri Lanka (GOSL) has taken an important decision to continue with the program into other landslides prone districts. In the absence of external assistance, the GOSL decided to fund all costs of the program in subsequent phases. The program now has stepped in to its 12^{th} year of operation (Phase III) and made remarkable progress by completing mapping in the priority areas of the four districts.

Landslide Studies and Services Division (LSSD) of NBRO has already produced a set of landslide hazard maps (1: 10,000) and database covering priority areas of the four districts in the central hill country. These maps and data would provide an essential input to the landslide risk management process. Heavy investment had been incurred to develop a scientific methodology of landslide hazard mapping/ identification. The landslide risk assessment, evaluation and treatment are the logical next steps in the landslide risk management process that will pave the way for covering the "know-how" on mapping into the "show-how" for utilization of benefits in the overall context of natural disaster mitigation.

2.0 Landslide Hazard Assessment/ Mapping

2.1 General

Landslide hazard mapping represents a scientific attempt to unfolding the causative factors which directly or indirectly influence slope stability and concatenate them to develop a criterion on the basis of which slopes could be graded in terms or their estimated degrees of instability, danger or hazard (Bhandari et al 1994).

2.2 Methodology of Landslide Hazard Mapping

The following two broad options were available at the start of the landslide hazard mapping:

- Direct mapping of landslide hazards based on geological, geomorphological and geotechnical investigations, and mapping by a single multidisciplinary team.
- State-of-nature (factor) mapping and integration of factor maps into landslide hazard maps.

The second option was selected for Sri Lankan landslide hazard mapping work and the major steps involved in a mapping are :

1. Identification of causative factors influencing instability in a given geological environment, investigation and mapping.
2. Short-listing of most relevant causative factors and consequent detailing out of the maps.
3. Holistic study of maps in the background of other related information and search for inter-relationships between the causative factors.
4. Figuring out the degrees of instability based on the criterion developed.
5. Field verification of hazard maps.

In the methodology adopted, the basic information were obtained though :

1. Desk studies including airphoto interpretation leading to production of maps of landform, landuse and management, and slope range and category.
2. Field surveys aided by photogrammetric studies leading to production of maps of former landslide and overburden deposits, bedrock geology and structure, location and hydrology.
3. Mapping of human settlements and infrastructure at risk through air photo interpretation, making use of available maps and information from the records of district authorities.
4. Socio-economic surveys

The desk and field studies were designed so as to produce seven (07) state-of-nature maps. There are Bedrock and Geology, Former Landslides and Overburden Deposits, Location and Hydrology, Slope Range and Category, Landform, Landuse and Management and Human settlement and Infrastructure (Figure 2).

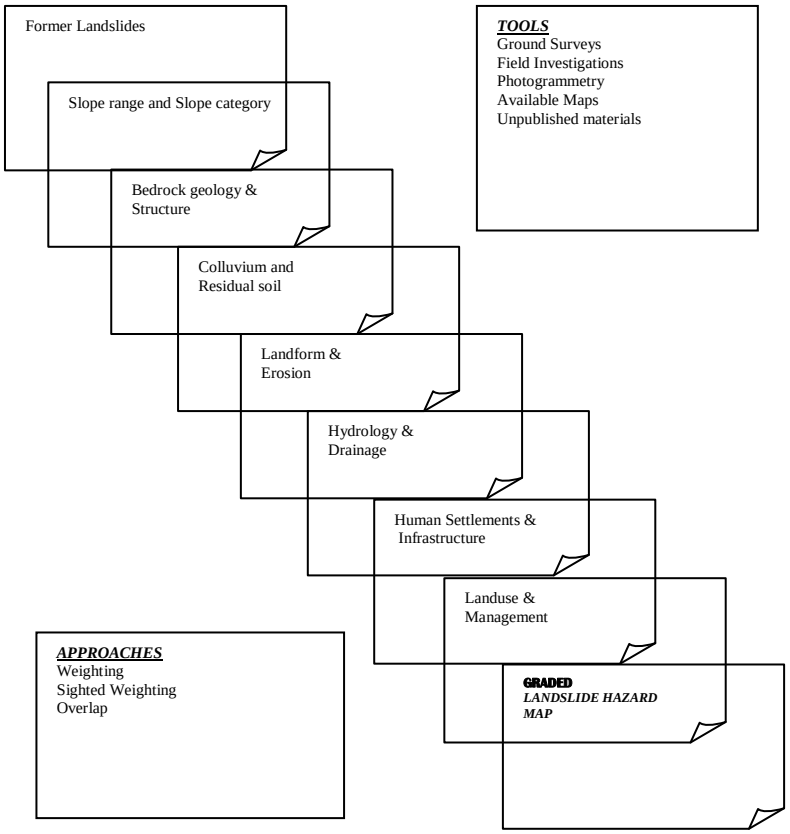

Figure 2 : Tools, Approaches and Integration of Factor Maps into a Graded Landslide Hazard Map

There was no rigid starting or termination point for carrying out both desk and field studies for the simple reason that they are intimately interrelated all the way. Air photo study had to be pursued throughout not only to add details to the maps but also to encourage checking of field maps. Most maps produced in the programme went through the process of checking at least once. In order to facilitate hazard mapping, the total area is divided into basic terrain units, called components, facets or grid cells. The grid cells of a fixed size have the disadvantage of often relating poorly to the geomorphologically meaningful slope units, distinguishable in the landscape.

Integration of factor maps required the highest value judgment in assigning scores, weighted scores or numerical ratings. Although it was not possible to obtain unanimous agreement on a highly subjective matter such as this one, attempts were made to arrive at decisions based on collective wisdom. Realising the inappropriateness of heavily relying on a single procedure, the methodology was modulated to accommodate the flexibility of separately making use of weighting approach, sighted weighting approach and overlap approach.

The method adopted laid emphasis on :

- Overlaying factor maps involving highly interrelated factors which promote or inhibit slope instability, for interpretation of hazard.
- Each category within each factor map was given a rating according to how much it promotes or inhibits landslide susceptibility.
- Factor maps were given similar ratings.

"Weighting Maps" are produced as the first step to have a feel of the hazard distribution (Froehlich et.al 1978). It draws heavily on preconceived and intuitive judgment on relative importance of different factors. In this procedure;

1. Weighting (relative importance) is given to different factors according to personal experience.
2. Maps are overlaid and ratings summed up for each resulting map unit.
3. Total ratings provide the basis for grouping in to the hazard categories.

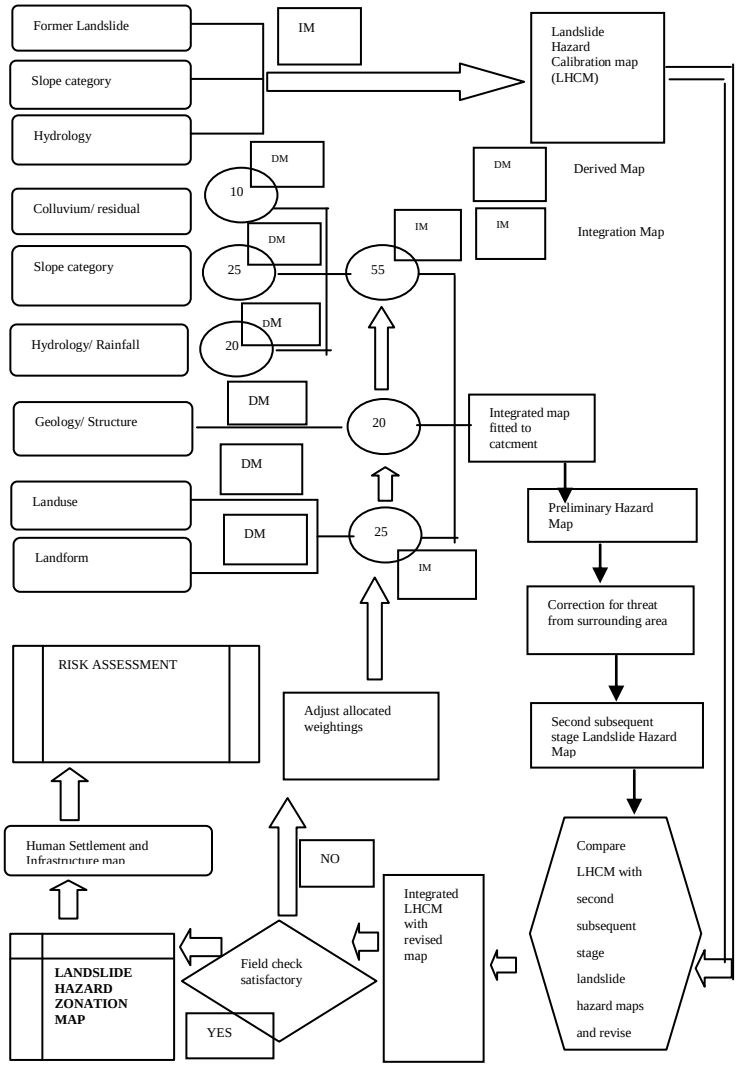

Figure 3 : Landslide Mapping Scheme in Sri Lanka

Sighted weighting is where ratings are improved by using information on former landslides as an aid to judging the weighing of the factor maps categories and of the maps themselves. Factor categories with low landslide densities are given lower hazard rating when compared with those with higher hazard rating.

The overlay approach requires mapping of each of the contributing factors separately and then overlaing the map units of each of the factor maps. The maps units that arise naturally from this overlay process become the units of assessment, e.g the combined hazard maps of Ives and Boris (1978).

The task of describing zonal significance of a landslide hazard map has been handled differently in different landslide hazard zonation programmes in the world. The zonal significance of Sri Lankan landslide hazard zonation map is shown in Table 1.

2.3 Achievements to- date and Future Directions

Of the seven landslides prone districts Badulla and Nuwara Eliya were the worst affected and therefore selected for initiation of landslide hazard mapping work (Phase I). Although the Phase I of the program ended in July 1995, the Government of Sri Lanka (GOSL) took an important decision to continue with the program into other landslides prone districts. In the absence of external assistance, the GOSL decided to fund all cost involvement of the program in subsequent phases. The program now has stepped in to its 12th year of operation and made a remarkable progress by completing mapping in four districts. In addition to graded landslide hazard zonation maps, state-of nature maps in 1: 10,000 scale the delivery of methodology for hazard zonation mapping and strengthening of the capacity of NBRO to handle landslide related matters can be seen as achievements of the project. Most notable feature of the project is the National Symposium on Landslides held in March 1994, which provided a forum for a gathering of large number of professionals and administrators as well as politicians.

At the final stage of Phase I, an attempt has been made to increase the demand for LHZ maps and also to demonstrate and test the capabilities of such maps. Meetings were held with user agencies and target beneficiaries and it was felt that the project should be restructured and reoriented towards establishment of sustainable long-term and short-term mechanisms for landslide disaster reduction in Sri Lanka. In this respect the project title has to be changed to suit the above task as, "Introduction of standards, guidelines and codes of practices for human settlement planning and site selection in hilly areas vulnerable to landslides".

Table 1. Zonal Significance of the Sri Lankan LHZ Map

Qualitative term used in zonation	Zonal Significance
Former Landslide	Landslides have occurred in the past. Known danger of landslides and therefore perennial threat to life and property exist in the area. All new construction should be prohibited and landuse and management degradation. Landslide redemption should be undertakan and early warning systems established at all problematic sites.
Most Hazardous Areas	Landslides most likely to occur. Danger and potential threat to life and property exist. No new construction will be permitted. Essential additions to the existing structures may be allowed only after thorough site investigation and adequate precautions, to be certified by specialist(s). Early warning systems should be established.
Hazardous Areas	Landslides to be expected. New construction should be discouraged, and improved landuse planning practices should be introduced to halt and reverse the process of slope degradation. All essential construction, redemption, and new projects would be subject to landslide risk assessment.
Moderately Hazardous Areas	Moderate level of landslide hazard exist. Engineered and regulated new construction and well planned cultivation can be permitted. Plans for construction should be technically certified.
Safe Areas	Landslides not likely to occur. No visible signs of slope instability or danger exist based on present state of knowledge. Limitations need not be imposed practically on well managed lands and engineered construction.

3.0 Landslide Risk Assessment – A Case Study

3.1 General

Hazard is confined to the expected occurrence of landslide, while risk involves the expected damage consequences of landslides (loss of life or injured persons, cost of property and infrastructure facilities etc.). The engineering analysis of landslide risk has essentially two components, the probability of occurrence and the resulting consequences. In Sri Lanka, very little has been done towards introducing scientific practices of landslide risk assessment delineating the degrees of hazard, identifying elements at risk, risk assessment and risk treatment. Landslide Studies and Services Division (LSSD) of NBRO has already produced a set of landslide hazard maps and Sri Lankan landslide database. These maps and data would provide an essential input to the risk assessment. The landslide hazard zonation map is a delineated area with different probability to initiate landsliding. But these maps are not available for every area of the landslide prone hill country. This study describes application of philosophy of landslide risk assessment with/without data from landslide hazard zonation map of the area.

The selected site for study at Yatinyantota is situated in the Kegalle district. Due to heavy rain, bank failures, cutting failures, gully erosion and small landslides occurred on 16 September 1997 at about 2.30 a.m. The recorded rainfall on 16th was 250mm/day. The unstable area covers about 2km stretch along the left side of the main road from Yatiyanthota town to Aliwatta village. It is easily accessible by Awissawella- Hatton main road (Location map Figure 4).

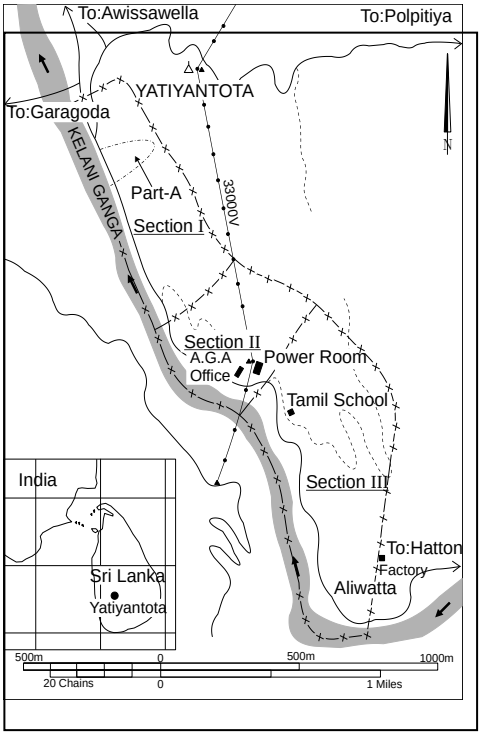

Figure 4 : Location Map of Study Area

Due to this failure, 4 houses were completely destroyed, 7 houses were partially damaged and 13 houses within the vulnerable area are threatened by future failures. However no human losses were recorded, perhaps as a result of awareness created about the causative factors and the importance of observance and constant vigilance during heavy rains by NBRO under LHMP. It is a known fact that the small-scale landslides can develop into a disastrous landslide event during monsoon seasons, if timely actions are not taken for remediation.

3.2 Landslide Risk Assessment in Sri Lanka

In Sri Lanka, very little has been done towards introducing scientific practices of landslide risk assessment delineating the degrees of hazard, identifying elements at risk, risk assessment and risk treatment. Therefore it is desired to develop a practical scientific method to evaluate landslide risk in central hilly areas and Arambepola (1998), Arambepola et al., (1999) and Abeysinghe et al., (1998), (2001), and (2002a,b) have conducted research for this purpose. Describing the product of risk assessment at a specific site or of elements at risk (property and persons) in qualitative terms (high risk, medium risk low risk, etc.) is not sufficient to indicate the severity of damages. Our experience is that it is more important to indicate the Rupee value of damages for policy and decision-makers (non technical) for them to get an idea of the damages occurred. This study describes framework for site-specific landslide risk assessment and can be used in future at any site of the landslide prone hilly areas of Sri Lanka.

Risk assessment can be applied in a number of areas (Ho et al., 2000). There are; (a) global risk assessment; to examine the scale of a problem and define the relative contribution of the different components to facilitate formulation of risk management policies and consideration of optimal resources allocation, (b) relative risk assessment; to determine the priority for follow-up action, (c) site-specific risk assessment; to evaluate the hazards and level of risk in terms of fatality (or economic or other loss) at a given site, and (d) preparation of hazard or risk mapping; for hazard zoning or planning control of a region or an area.

Site-specific risk assessment facilitates the assessment of whether the risk levels at a specific site are acceptable and assists in the determination of whether a proposed development should be permitted, and in the evaluation of cost effectiveness of mitigation measures, etc. The application of a site-specific quantitative risk assessment will need to be supported by the detailed examination of landslide trigger factors, mechanisms and mode of failure and debris run-out for the results to be sufficiently accurate.

The overall framework for quantitative risk assessment of slopes and landslides is general and multidisciplinary, consisting of the following activities; (a) hazard identification and probability of occurrence, (b) identification of the elements at risk, (c) estimation of vulnerability of the elements at risk, and (d) calculation of total risk.

In the overview paper of landslide risk management by Fell and Hartford (1997), the definition of total risk (R_t) is expected from the number of lives lost, persons injured, damage to property and disruption of economic activity. It is a product of specific risk (R_s) and element at risk (E) over all landslides and potential landslides in the study area, given as follows:

$$R_t = \sum R_s \times E \tag{1}$$

Specific risk (R_s) is product of the annual probability of occurrence (P_a) and the vulnerability (V) for a specific element at risk, given as:

$$R_s = P_a \times V \tag{2}$$

Combining Eqs. (1) and (2) yields the following equation;

$$R_t = \sum P_a \times V \times E \tag{3}$$

From the morphological characteristics, landslide can be divided into four major areas. There are head region, main body, foot and toe. Total risk is the sum of the risk on each area of the landslide and is given as equation (4);

$$R_t = \sum_{i=1}^{n} R_i \tag{4}$$

n – Number of areas considered in landslide (here, n=4)

$$R_t = R_1 + R_2 + R_3 + R_4 \tag{5}$$

Here, R_t is total risk over all landslide area, R_1 is total risk over head region of the landslide ($R_{t\text{-}Head}$), R_2 is total risk over body of the landslide ($R_{t\text{-}Body}$), R_3 is total risk over foot of the landslide ($R_{t\text{-}Foot}$) and R_4 is total risk over toe of the landslide ($R_{t\text{-}Toe}$).

Equation (5) can also be written as:

$$R_t = R_{t-Head} + R_{t-Body} + R_{t-Foot} + R_{t-Toe} \tag{6}$$

From equation (3) and (6), following equation is obtained as:

$$R_t = \begin{Bmatrix} \left(\sum P_a \times V_{Head} \times E_{Head}\right) + \left(\sum P_a \times V_{Body} \times E_{Body}\right) + \\ \left(\sum P_a \times V_{Foot} \times E_{Foot}\right) + \left(\sum P_a \times V_{Toe} \times E_{Toe}\right) \end{Bmatrix} \tag{7}$$

Here, R_t is annual total risk over the whole landslide area, P_a is the annual probability of hazardous event (the landslide), V_{Head}, V_{Body}, V_{Foot} and V_{Toe} are vulnerability of the elements at risk on respective areas of the landslide, E_{Head}, E_{Body}, E_{Foot} and E_{Toe} are elements at risk on respective areas of the landslide.

The elements at risk (E) can be divided to two major groups as : property and person. Also the element at risk (E) can be quantified by placing a Sri Lankan rupee value or some other form of value (U.S. Dollar or Japanese Yen) on them. Then risk (R) becomes a risk cost (R_c) and total risk (R_t) become a total risk cost ($R_{t\text{-}c}$). In here $R_{t\text{-}c}$ is the annual total risk cost, or annualized total risk cost, of the expected losses from the landslide hazard and equation (7) can also be written as:

$$Rt-c = \begin{Bmatrix} \left(\sum P_a \times V_{Head(property)} \times E_{Head(property)} + \sum P_a \times V_{Head(person)} \times E_{Head(person)}\right) + \\ \left(\sum P_a \times V_{Body(property)} \times E_{Body(property)} + \sum P_a \times V_{Body(person)} \times E_{Body(person)}\right) + \\ \left(\sum P_a \times V_{Foot(property)} \times E_{Foot(property)} + \sum P_a \times V_{Foot(person)} \times E_{Foot(person)}\right) + \\ \left(\sum P_a \times V_{Toe(property)} \times E_{Toe(property)} + \sum P_a \times V_{Toe(person)} \times E_{Toe(person)}\right) \end{Bmatrix} \tag{8}$$

Here, $R_{t\text{-}c}$ is the annual total risk cost over the whole landslide area, P_a is the annual probability of hazardous event (the landslide), $V_{Head(property)}$, $V_{Body(Property)}$, $V_{Foot(property)}$ and $V_{Toe(property)}$ are vulnerability of the properties which are on respective areas of the landslide, $V_{Head(person)}$, $V_{Body(Person)}$, $V_{Foot(person)}$ and $V_{Toe(person)}$ are vulnerability of the persons who are live on respective areas of the landslide, $E_{Head(property)}$, $E_{Body(property)}$, $E_{Foot(property)}$ and $E_{Toe(property)}$ are elements at risk (property) on respective areas of the landslide. $E_{Head(person)}$, $E_{Body(person)}$, $E_{Foot(person)}$ and $E_{Toe(person)}$ are elements at risk (person) on respective areas of the landslide.

3.3 Hazard Identification and Probability of Occurrence

Hazard identification and probability of initiate landsliding of an area could be determined using the graded landslide hazard map. The currently available landslide hazard zonation maps being on the scale of 1:10,000 are not sufficiently detailed for utilization in assessing hazards or risks in location specific situations in hilly areas of Sri Lanka. Also these maps are not available for each area of the landslide-prone hilly areas. Therefore in this study following simple landslide hazard assessment method (field score evaluation) was introduced and could be used at any location specific site of Sri Lanka.

Though a reconnaissance survey carried out by NBRO in early 1986, over 200 landslide locations were subsequently recognized in the hilly areas of Sri Lanka. For detailed investigation in pursuance of the landslide research programme, 64

slide locations were selected. The principal objective of the research was the identification factors contributing to landslides in Sri Lanka and their degree of contribution for the landslide process. One of the other objectives of the landslide research project is to develop a methodology to identify areas of potential landslide hazards which is not very expensive and less time consuming to evaluate (A Study of Landslides in Sri Lanka, 1990).

Using the data base (64 landslides) developed under this project the causative and contributory factors for slope instability in Sri Lanka were identified by carrying out analyses of the database information on these factors. The major factors are bedrock geology and structure, overburden deposits, slope angle, hydrology, and landform and landuse management. Sub-factors and sub factor elements that cause slope instability were also identified. The above landslide database was used to evaluate the numerical rating of each causative or contributory parameter for each site. For each parameter, a numerical rating was given depending on its severity. These numerical ratings of each parameter were combined together in a formula to determine the combined effect on slope instability. The value thus determined is called the landslide hazard factor *H*.

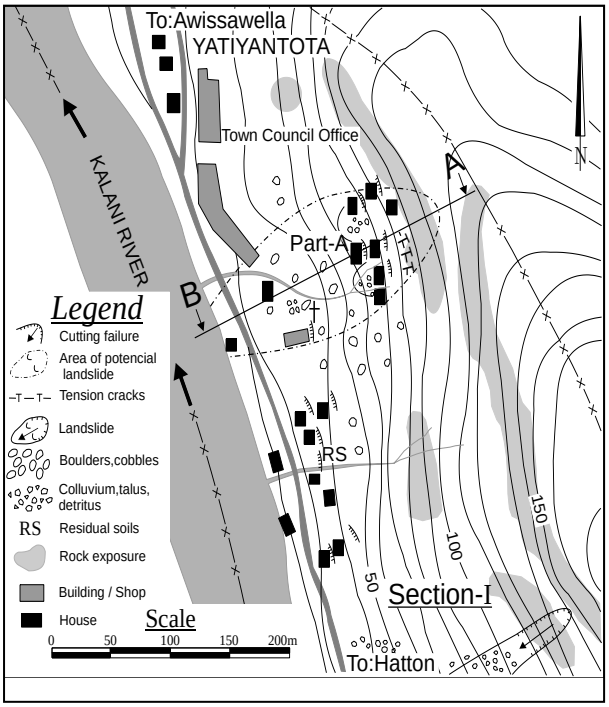

Figure 5 : Potential Landslide Hazard Area at Yatiyantota

For a given weighting system and a given set of formula the distribution of values was studied. The weighting or numerical rating system and the formulae were changed until the standard deviation of the distribution of *H* becomes a minimum value. The results of the study are based on the developed method for landslide hazard zonation mapping in Sri Lanka, which was in use since 1995 (Manual of Landslide Hazard Zonation (1995). The model value of the *H* distribution (when normalized) was then selected as the critical value of *H*.

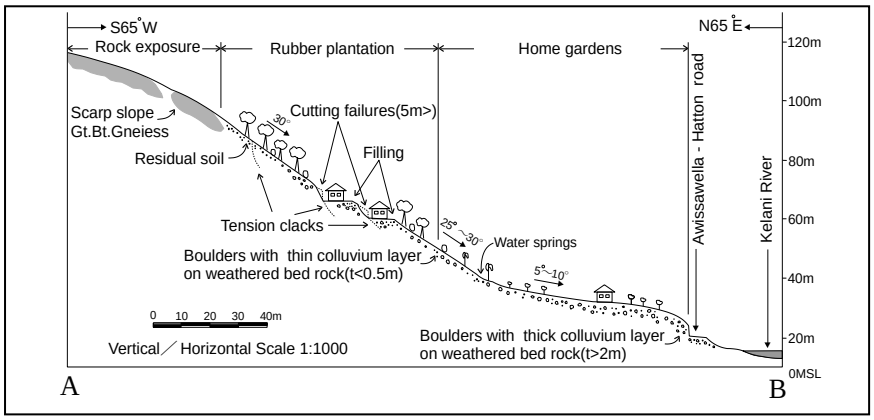

Figure 6.Generalized Cross Section of in Study Area (Section A-B in Figure 5)

The field scoring method proposed in this study for landslide hazard evaluation at specific site is shown in Table 2. It is based on the contributory parameters for landsliding and consider on major factors, sub factors and sub factor elements. A relative weight (degree of importance) was determined almost similar to already developed and being used for landslide hazard zonation mapping programme in Sri Lanka (Manual of Landslide Hazard Zonation, 1995).
The study area of the unstable slope on which houses are located was divided into 3 geomorphologic sections according to the slope angle and direction (Section I, II & III; Figure 4). Basic data for the hazard evaluation in each section of the study area were obtained by field investigation and are compiled on the score columns in Table 2. By summing up the scores, landslide hazard (H) can be quantitatively evaluated. The evaluation indicated that the Section (I), Section (II) and Section (III) have a hazard (H) of 77, 61 and 62, respectively. The relationship between hazard and qualitative terms used in hazard evaluation (Manual of Landslide Hazard Zonation, 1995) is shown in Table 3. According to Table 2, Section (I) was identified as the most hazardous area and Sections (II) and (III) were hazardous areas. Also the result of preliminary field investigation indicated that, Part (A) area of Section (I) was the most vulnerable to future disaster due to landslide hazard. This area was selected for further studies and assessment of risk. The detailed field investigation helped to identify probable landslide boundary, failure mechanism and type as a landslide with debris flow. In Figure 5, the potential landslide area Part (A) in Section (I) is shown. Figure 6 shows the cross section A-B of the Part (A) area.

Assessing the probability of landsliding (particular for an un-failed natural slope) is difficult as it involves much uncertainty and judgments. In recognition of this uncertainty, it is the common practice to report the probability of landsliding using qualitative terms such as very likely, likely, unlikely or very unlikely. When qualitative terms are used to describe likelihood of landslides, it should be linked with indicative probability. An example of this empirical link is given in Table 3 and the indicative value may vary by an order of magnitude. $P_a > 1/100$ (10^{-2}) indicates the hazard is imminent, and well within the lifetime of a person or typical structure. The landslide is clearly identifiable with fresh signs of disturbance on the ground. P_a of 1/1000 (10^{-3}) indicates that the hazard can happen within the approximate lifetime of a person or typical structure. P_a of 1/10000 (10^{-4}) indicates that the hazard within a given lifetime is not likely, but possible. P_a of 1/100000 (10^{-5}) indicates that the hazard is of uncertain significance.

Table 2 : Field checklists for ranking of landslide hazard (H)

Bed rock geology and Structure (20)	Lithology (8)	0 1 3 5 8	Marble Weathered rock Granite, Gt.bt.gn, all others Charnockite, Granulite, NBE Quartzite
	Amount and direction of Dip (4)	0 1 2 3 4	Dip and scarp 70°-90° Dip and scarp 55°-70° Dip 10°-30°, scarp 45°-55°, inter. Dip 0-10°, scarp 30°-45° Dip 30°-55°, scarp 0-30°
	Deviation angle (6)	0 2 4 6	25°-120° 10°-25° or 120°-155° 155°-180° 0-10°
	Discontinuities (2)	0 2	Absent Present
Overburden deposits (10)	Soil Thickness (10)	0 2 8 9 10	Bed rock Coll < 1m, overburden < 2m Coll 1-3m, overburden 2-8m Coll 3-8m, overburden >8m Coll > 8m, overburden >8m
Slope angle (25)	Slope Angle (25)	5 15 25 20 10	>40° 31°- 40° 17°-31° 11°-17° 0-11°
Hydrology (20)	Piezometer level (ground water table) (20)	3 7 10 15 20	Below slip plane Above slip plane Between ground level & slip plane At ground surface Artesian or above ground level
Landform and landuse (25)	Landform (15)	3 8 10 12 15	Simple slope (no previous slides) Simple slope with surface cracks Old slip but modified by erosion New slip now stable no erosion Recent slip, erosion at toe
	Landuse (10)	1 2 3 5 7 8 10	Natural woods (undisturbed) Cleared and cultivated well Cleared for pasture land Disturbed by cattle Controlled construction Disturbed by construction but precautions taken Heavy construction
100	Total score	77%	

Table 3. Relationship between Hazard and Probability of Landslide

Hazard Range	Qualitative Term Hazard Zonation	Probabilistic Criterion Grade	Indicative Annual Probability
H≤40	Safe Areas	Very Unlikely <5%	10^{-5}
41≤H≤55	Moderate Hazard	Unlikely 5-20%	10^{-4}
56≤H≤70	Hazard	Likely 20-80%	10^{-3}
71≤H≤100	Most Hazard	Very Likely >95%	10^{-2}

According to Table 3, Part (A) area of the Section (I) in the most hazardous area, and has a probability for landsliding > 95%, (which is very likely) and the indicative annual empirical probability for landslide is $>10^{-2}$. Similar slopes (geology, geomorphology, climate, etc.) in most hazardous areas (identified using available landslide hazard zonaton map) close to study area, and the landslide history of the last 5 years were studied, which showed that 25 slopes failed within this 5year period. Therefore statistically, Part (A) area in the most hazardous area with probability of landsliding as very likely, and an annual probability of failure of $0.5x10^{-2}$ may be applied. The quality and accuracy of the result depends on both the knowledge (the ability to recognize what is similar slope) and experience (knowledge about the performance over time of many similar slopes) of the assessor.

3.4 Elements at Risk

In the overview paper of the IUGS working group on landslides (1997), the definition of elements at risk means the population, buildings and engineering works, economic activities, public services utilities and infrastructure in the area potentially affected by landslides. In more detail, the elements at risk will include; (a) property, which may be subdivided into portions relative to the hazard being considered, (b) people, who either live, work, or may spend some time in the area affected by landsliding, (c) services, such as water supply or electricity supply and (d) roads and communication facilities. The element at risk (*E*) can be quantified by placing a Sri Lankan rupee value or some other form of value (U.S. Dollar or Japanese Yen) on them.

When the probable landslide boundary is superimposed with the human settlements and infrastructure of the area, it was observed that (Part (A) of Section I) following persons and properties are vulnerable to future landslide events (Fig. 5 and Table 4) : 107 persons, 3 retail shops, 9 houses, a church, a foot path, a telephone exchanger and a road approximately 125m long. The property value is taken by considering the land, type and condition of the property. Although humans cannot be valued, since the study required a figure to calculate the amount of Rupees 150000.00 are considered. It is an average amount paid by insurance.

Table 4 : Elements at Risk in Yatiyantota Potential Landslide

Area of the landslide	Element at risk	Property value (Rs.)	Person Value (Rs.)
Head region	2 houses/ 7 persons	1000000	7 x 150000
Main body	5 houses/ 20 persons 50m footpath	5000000 100000	20 x 150000
Foot	1 house/ 5 persons 20m foot path 2 shops/ 20 persons 1 church/ 50 persons Telephone Exchanger	700000 50000 3000000 2000000 1000000	5 x 150000 20 x 150000 50 x 150000
Toe	1 house/ 3 persons 125m highway	700000 1250000	3 x 150000 2 x 150000

3.5 Estimation of Vulnerability

Vulnerability (*V*) is the degree of loss to a given element or set of elements within the area affected by the landslide hazard. It is expressed as a scale of 0 (no loss) to 1 (total loss). For property, the loss will be the value of the damage relative to the value of the property; for persons, it will be the probability that a particular life will be lost, given the persons is affected by the landslide (IUGS working group on landslides, 1997).

Table 5 : Estimation of Landslide Vulnerability for Property and Persons

Area	Factors	$V_{Property}$	$V_{Persons}$
Head region	High velocity, medium depth, little warning, short escape distance	0.7	0.3
Main body	High velocity, high to medium depth, little warning, long escape distance	1.0	0.5
Foot	Medium velocity, debris accumulation, some warning, short escape distance	0.4	0.01
Toe	Low velocity, more warning, short escape distance, debris flow< mud flow	0.1	0.001

Although the state of the art for identifying the elements and their economic value is relatively well developed, the state of the art for assessment of vulnerability is in general primitive. This may be determined in terms of a damage function or more simply estimated single values, which are likely to have been determined from previous experience or judgment (IUGS working group on landslides, 1997). Vulnerabilities of property and persons in the study area were estimated based on the author's field experience (about 10 years) in the past landslide disaster history of similar slopes in Sri Lanka. The assumed values are given in Table 5. It is important that persons with training and experience in landsliding and slope failure process are involved in this estimation because under-or over-estimation will control the outcomes of the analysis. The vulnerability is affected by the nature of the affected part, whether it is head, body, foot or toe of the landslide, and the nature of the element at risk (property or persons). The velocity of movement, also affects the vulnerability, with higher velocities usually leading to greater vulnerability. This can lead to different degrees of damage on or in the travel path (from head region to toe area) landslide. The vulnerability of lives and property damage may also be quite different. A house may have similar and high vulnerability to a slow and a rapid landslide, but persons living in the property may have a low vulnerability to the slow landslide (they can move out of the way) but a higher vulnerability to the rapid landslide.

3.6 Calculation of Total Risk

$R_{t\text{-}c}$ is the annual Total Risk cost, or annualized total risk cost, of the expected losses from the landslide hazard and could be calculated from the equation (8), using data from section 3.3, 3.4 (Table 4) and 3.5(Table5).

$$Rt-c=\left\{\begin{array}{l}\left(\sum P_a \times V_{Head(property)} \times E_{Head(property)} + \sum P_a \times V_{Head(person)} \times E_{Head(person)}\right)+\\ \left(\sum P_a \times V_{Body(property)} \times E_{Body(property)} + \sum P_a \times V_{Body(person)} \times E_{Body(person)}\right)+\\ \left(\sum P_a \times V_{Foot(property)} \times E_{Foot(property)} + \sum P_a \times V_{Foot(person)} \times E_{Foot(person)}\right)+\\ \left(\sum P_a \times V_{Toe(property)} \times E_{Toe(property)} + \sum P_a \times V_{Toe(person)} \times E_{Toe(person)}\right)\end{array}\right\}$$

$$Rt=c=\left\{\begin{array}{l}\left[(0.05\times 0.7\times 1000000)+\{(0.05\times 0.3\times 150000)7\}\right]+\\ \left[\{0.05\times 1.0(5000000+100000)\}+\{(0.05\times 0.5\times 150000)20\}\right]+\\ \left[\begin{array}{l}\{0.05\times 0.4(700000+50000+3000000+2000000+1000000)\}\\ +\{(0.05\times 0.01\times 150000)75\}\end{array}\right]+\\ \left[\{0.05\times 0.1(700000+1250000)\}+\{(0.05\times 0.001\times 150000)5\}\right]\end{array}\right\}$$

$$R_{t-c}=0.5311625 Rs.Million$$

Therefore annual total risk cost, or annualized total risk cost, in the potential landslide area or Part (A) of Section (I) is 0.5312 Million Rupees (In December 2004 general currency exchange rate was : 100.00 Sri Lankan Rupees equal to 1U.S $)

The value of expected total risk cost due to landslide disaster may be of interest to policy makers or decision-making authorities (Provincial Councils, Local Government Institutions, Insurance Companies etc.) involved in development work in the area. It may assist in the designing of cost effective solutions and mitigation actions for the area. It is also expected to help non-technical decision-makers to assess the situation before taking appropriate future measures.

3.7 Limitations of the Landslide Risk Assessment

As seen in the study, there are a number of limitations to risk analysis and assessment for slopes and landslides;

- The judgments, and content of the inputs may well result in values of assessed risks with considerable inherent uncertainty. More experience and understanding of the process may improve the reliability of the assessment.
- The variety of approaches that can reasonably be adopted to assess the landslide risk can result in significant differences in the outcome if different practitioners consider the same problem separately.
- Revisiting an assessment can lead to significant change due to increased data, by application of a different method or change of the circumstances.
- The inability to recognize a significant hazard and the consequential underestimation of the risk.
- The methodology is currently not widely accepted and thus sometimes there may be an aversion to its application.

4.0 Concluding Remarks

It is an accepted fact that the graded landslide hazard maps will play an important role in site selection and developing and planning of infrastructure within the hill country of Sri Lanka in the future.

The methodology for risk assessment given in this paper will facilitate determination of risk through scientific analysis of landslide hazards in future. The expected total risk due to landslide disaster, cost for mitigation actions and loss prevention costs may also be calculated through the given methodology. It is expected to help non-technical decision-makers to assess the situation before adopting appropriate future measures. This methodology may be used for assessment of the risk in any landslide prone area in central highlands provided that sufficient basic data is available for assessment. The application areas of proposed methodology are very wide and decision-making by authorities (Provincial Council, Local Government Institutions, Insurance Companies, Lending Institutions etc) as well as individuals (effected families, victims, businessmen, etc) may be based on results obtained through the assessments using the proposed methodology.

Development of a culture for risk analysis before commencement of major infrastructure development projects and establishment of human settlements in landslide prone areas based on the risk criterion is desired to be considered as an essential factor for sustainable development in areas prone to landslides in the hill country of Sri Lanka.

5.0 Acknowledgements

This paper forms a part of the research study conducted by the main author for doctoral studies at the Saga University, Japan, under the Monbusho scholarship (2000-2004) awarded by the Japanese Government. Authors wish to thank Director General - NBRO for the permission granted to use published and unpublished data for preparation of this paper. The constant guidance and advice provided by Mr. N.M.S.I. Arambepola, former Head- LSSD/ NBRO, and Dr. Jagath Gunatilake, Department of Geology, University of Peradeniya are acknowledged with profound gratitude. Authors also wish to acknowledge with gratitude the cooperation and assistance extended by all the members of the Landslide Hazard Mapping Project of NBRO.

6.0 REFERENCES

Cooray, P.G. (1978): Geology of Sri lanka, Proc. Regional Conference on Geology and Mineral Resources of South East Asia, Bangkok, 14-18 Nov., pp.701-710.

Berger, A.R. and Jayasinghe, N.R. (1976): Precambrian Structure and Chronology in the Highland Series of Sri Lanka, Precambrian Research13, pp.559-576.

Varnes, D.J. and the Inter. Assoc. of Engineering Geology Commission on Landslides and other Mass Movements (1984): Landslide Hazard Zonation: A Review of Principals and Practice. Natural Hazards, vol.3, Paris, France, UNESCO, pp.63.

Whitman, R.V. (1984): Evaluating Calculated Risk in Geotechnical Engineering. ASCE Jour. Geotechnical Engineering, 110(2), pp.145-188.

Einstein, H.H. (1988): Special Lecture, Landslide Risk Assessment. Proc. 5th Int. Symp. on Landslides, Lausanne, Switzerland, A.A Baalkema, Rotterdam, The Netherlands, Vol.2, pp.1075-1090.

Morgan, G.C., Rawlings, G.E. and Sobkowicz, J.C. (1992): Evaluating Total Risk to Communities from Large Debris Flows. In Geotechnique and Natural Hazards. Proc. Geohazards-92 Symposium, BiTech Publishers, Canada, pp.225-236.

Fell, R. (1994): Landslide Risk Assessment and Acceptable Risk, Canadian Geotechnical Journal, 31, pp. 261 – 272.

Ho, K., Leroi, E. and Roberds, B. (2000): Quantitative Risk Assessment: Application, Myths and Future direction. Proc. GeoEng2000, Melbourne, Australia, 19-24 Nov., pp.269-312.

Einstein, H.H. (1997): "Landslide risk – Systematic Approaches to it's Assessment". Proc. 5th Int. Workshop on Landslide Risk Assessment, Honolulu, Hawaii, pp.25-50.

Fell, R. and Hartford, D. (1997): Landslide Risk Management, in "Landslide Risk Assessment" Cruden and Fell (eds.), Balkema, Rotterdam, pp. 51-110.

Australian Geomechanics Society (2000): "Landslide Risk Management Concepts and Guidelines". Australian Geomechanics Society, Sub-Committee on Landslide Risk Management, Australian Geomechnics, Vol.35, pp.49-92.

Arambepola, N.M.S.I. (1998): Risk Assessment and Environmental Protection in Landslide Prone Areas of Sri Lanka, Project Report submitted to National Science Foundation under the Research Grant No. RG/97/NR/01, Vol. I, II and III.

Arambepola, N.M.S.I., Abeysinghe, A.M.K.B. and Bandara, R.M.S. (1999): Risk Assessment for Landslides in the Central Hills of Sri Lanka. Abst. Proc. International Symposium on Eng. Geol. Hydrogeology and Natural Disasters with Emphasis on Asia, Kathmando, Nepal, 28-30 Sep. pp.250.

Abeysinghe, A.M.K.B., Bandara, R.M.S. and Arambepola, N.M.S.I. (1998): Development of a Methodology for Risk Assessment in Landslide-prone areas of Sri Lanka – A Geotechnical Approach. Proc. Workshop on the Role of R & D Institutions in Natural Disaster Management, Colombo, Sri Lanka, 10-11th September, pp.10.1-10.5.

Abeysinghe, B., Iwao, Y. and Gunatilake, J. (2001): Risk Assessment of Landslide Vulnerable Slopes in the Hill Country of Sri Lanka. Proc. 3rd International Summer Symposium, Japanese Society of Civil Engineers (JSCE), Tokyo, Japan, 8th August, pp.217-220.

Abeysinghe, B., Iwao, Y., Gunatilake, J. and Arambepola, N. (2002a): Landslide Hazard Mapping Programme of the Landslide Prone Hill Country of Sri Lanka, Proc. 9th Congress Engineering Geology for Developing Countries, Durban, South Africa, 16-20 Sep., Extended Abstract Vol. pp. 247 (Full paper in CD Vol.).

Abeysinghe, B., Iwao, Y. and Arambepola, N. (2002b): Landslide Hazard and Risk Assessment on Hill Country of Sri Lanka. Proc. Regional workshop on Best Practices in Disaster Mitigation – Lessons Learned from AUDP and other initiatives, Bali, Indonesia, 24-26 September, pp. 438-443.

Ho, K., Leroi, E. and Roberds, B. (2000): Quantitative Risk Assessment: Application, Myths and Future direction. Proc. GeoEng2000, Melbourne, Australia, 19-24 Nov., pp.269-312.

Manual on Landslide Hazard Zonation (1995): Landslide Hazard Zonation Mapping Project (LHMP), SRL/89/001, prepared by the National Building Research Organisation, Colombo, Sri Lanka.

IUGS Working Group on Landslides, Committee on Risk Assessment (1997): "Quantitative Risk Assessment for Slopes and Landslides – The State of the Art", Honolulu, Feb., pp.1-10.

Bhandari, R.K., Herath, N., Thayalan, N. 1994. Landslide Hazard Mapping in Sri Lanka, A Holistic Approach. Proceedings of the National Symposium on Landslides in Sri Lanka, Vol. 1, 271-284pp.

Vitanage, P.W. (1985): The Geology, Structure and Tectonics of Sri Lanka and South India, Recent advances in the Geology of Ceylon; Inter. Center for Training and Exchanges in the Geosciences, Paris, Occasional Publication No. 6, pp.5-15.

Use of Soil Nailing Technique for Stabilization of Slopes

S.A.S. Kulathilaka, Senior Lecturer, Department of Civil Engineering, University of Moratuwa
D.C.A. Mettananda, Research Student, University of Calgary, Canada
(Formally Research Student – University of Moratuwa

ABSTRACT: Soil Nailing technique is widely used very successfully in many countries to stabilize slopes and embankments with many proven advantages including low cost. This research was aimed at studying the behavior of soil nailed structures in Sri Lankan conditions and to find the improvement achieved in the factor of safety.

Limit equilibrium methods were incorporated in the analysis and the design of soil nailed structures. Two analytical models were developed using Bishop's method and Janbu's simplified method to analyze the stability of the soil mass and assess the improvements achievable with soil nailing. Laboratory model slopes were then constructed and they were loaded to failure. Data relating to the failure surfaces were back analyzed using the analytical models. In the final phase, an attempt was made to design soil nail arrangements for some critical slopes in the hill country.

Model test results indicated that a remarkable increase of the stability could be obtained by soil nailing, and that the pullout resistance of nails in lateritic soils are greatly influenced by the moisture content. Also, disturbances during driving of the nails reduced the pullout resistance of the driven nails.

1.0 Current State of the Art of Soil Nailing Technique

Soil Nailing is a practical and cost-effective technique to stabilize slopes and excavations through the introduction of reinforcements into the soil mass. Nails, generally made of steel, are installed in a cut face in original ground on a pattern which may or may not be varying with wall height; the nails are connected by steel mesh or shotcrete facing to hold the soil near the cut face in place between the nails. Sometimes precast or cast-in-place concrete facades or seeded mats are used to improve the appearance of the facing for permanent facilities. The main difference between nailing and other ground reinforcing techniques such as reinforced earth is that the nailing is done for in-situ ground in a top down process, while the other reinforcement techniques are used to reinforce new constructions in a bottom up process.

The nails strengthen the ground by helping the soil to resist deformations. As the ground deforms, the nails share the load with the soil, gradually becoming more stressed in tension from an initially nominal stress level at installation. As the soil deforms, the nails become tensioned to the extent that is necessary to arrest the deformations and stabilize the soil. The nails are therefore a technique of passive stabilization unlike tiebacks, which are pre-tensioned at installation.

1.1 Historical Development

The first Soil Nailed slope available in literature is the steel bar reinforced railroad cut slope near Versailles, France and it was constructed in 1972. The slope was of an angle 70^0 and a total of 12 000 m^2 of face had been stabilized by over 25 000 steel bars grouted into predrilled holes up to 6m long [Bruce and Jewel 1986]. Thereafter, the technique became popular in many other countries including USA, Canada, UK, Australia, Hong Kong, Japan and Germany.

Soil nailing is a recent development and hence, it has not yet been applied widely in Sri Lanka. However, this technique had been used successfully in stabilizing one embankment at the site of famous Watawala landslide in 1995.

1.2 Applications of Soil Nailing

Soil Nailing has been used successfully in temporary and permanent applications, in new and remedial construction, and in rural and urban settings. The categories of applications can be identified as Excavation Support, Stabilization of Slopes and Retaining Wall repairs.

1.3 Benefits and Limitations

Several factors have contributed to the growing popularity of soil nailing as a construction technique. They include low cost, use of light construction equipment, construction flexibility, high performance and compatibility with the environment.

From the records of previous applications in Europe and USA, it has been proved that soil nailing can provide a saving of 10% to 30%, in cost compared to an anchored diaphragm wall.

The technique has certain limitations as well. It is not applicable for soft clays. The low frictional resistance of soft clay would require very high density of insitu reinforcement of considerable length to ensure adequate levels of stability. If the groundwater percolates through the face, the unreinforced soil will slump locally on initial excavation, making it impossible to

establish a satisfactory shotcrete skin. In the case of an excavation, soil of height of about 1 - 2m should be able to stand for a few hours unsupported until the shotcreting and nailing is completed.

2.0 Elements in the System and the Construction Technology Used

Main components involved in soil nailed retaining structures are the in-situ soil, nails and the facing.

2.1 Insitu Soil

Insitu soil forms the main structural element in a nailed wall. Hence, a combination of conventional and specialized geotechnical investigation and testing is necessary to obtain the characteristics of the soil. Conventional exploration (i.e., boring, sampling, and laboratory soil testing) is needed to characterize the soil deposit with respect to: geological origin and stratification; soil density and shear strength; groundwater level and flow regime; presence of running sands, presence of boulders and other geologic anomalies. Specialized testing is needed primarily to determine the ultimate pull-out resistance of prototype nails.

2.2 Nails

Nails are usually mild steel or high strength steel bars. They can be either driven into the ground or placed in pre-bored holes and contained with a suitable grout.

A wide range of reinforcing elements can be used as driven reinforcement. Generally, simple and low cost mild steel bars, having a yield strength of 250 N/mm^2 are used. Their diameters vary from about 12mm to 25mm. Tensile strength of these elements is relatively low and it is of the range of 45 to 150 kN. Generally they are spaced closely (about 2 bars per square meter) in a nailed retaining structure.

A rapid method of driving nails is by the use of a small vibropercussion hydraulic hammer. However, another new driving method employs a system that can grout the nail at high pressures while simultaneously driving it into the ground. The grout lubricates the nail as it is driven, improving drivability as well as the character of the soil near the nail [Xanthakos et. al. (1994)].

The reinforcement inserted in pre-drilled holes and subsequently grouted are made of high strength steel with a yield strength of 460 N/mm^2. Diameter varies from 12mm to 38mm. They are more expensive than mild steel bars. Generally, one bar is placed in a borehole of 100mm to 150mm diameter with spacing varying from 1m to 3m. They are normally grouted into the boring by gravity rather than high pressure. Specially ribbed bars can be used to improve the adherence with the grout.

Common methods of installation are auger drilling, rotary or rotary percussive drilling and duplex drilling. Air, water or a dense fluid may be utilized as a drill flush, if required. However, the use of bentonite is not recommended because of the possibility of leaving a smear in the hole, which can diminish the load transfer capacity between the grout and the soil. Grouting should be carried out from the bottom of the hole.

The attachment of grouted reinforcement to the facing (mesh or shotcrete) is generally made by bolting the bars to a square steel plate of thickness 14mm - 20mm and width 300mm to 400mm. The attachment of driven bars to the facing is generally made by cladding or another suitable method.

Corrosion of steel nails is a main factor that decides the life of a soil nailed wall. Many authors have discussed various methods of protecting nails against corrosion. One approach is a double protection, in which the nail bar is inserted into a corrugated plastic sheath and the space in between is grouted, for permanent structures. Another approach is to use epoxy-coated steel bars with a minimum of 35mm of cement grout around the steel bar. However, Hewitt and Haustorfer (2000) states that the majority of soil nail wall constructions in Australia up to date were done with hot dip galvanized bars installed in a cement grout filled borehole. However, some proprietary systems have also been developed in this regard. The use of high carbon fibre nails is another recent development to prevent corrosion in nails.

2.3 Facing

The facing must be structurally designed to take into account the modest bending moment and tensile stresses induced by soil pressures and nail forces. Common facing types include welded mesh facing, shotcrete facing, prefabricated panel facing and hydroseeded facing.

Most common facing method is the application of shotcrete. Generally, shotcrete layer is about 100~300mm thick, and may or may not be reinforced. If reinforced, welded wire meshes of diameters ranging from 6mm to 10mm are utilized. Ortigao et. al. (1995) suggest that steel or synthetic fibres mixed with the shotcrete can be used to replace the steel mesh. It has the advantages of saving time, labour and quantity of concrete.

Hydroseeding is the most recently introduced method of facing, and this has become very popular due to its ability to blend with the environment. Final surface obtained in this method is an aesthetically pleasing greenish grassy surface, which gives the slope a natural look. Different methods have been employed by different contractors to obtain a horticultural environment. They include spraying of a site-specific mix onto the front of a hessian, use of a pre-seeded hessian mat and soil panel system.

3.0 Methods of Analyses

The existing design methods for soil nailed retaining structures can be broadly divided into two categories, viz. Limit Equilibrium Design Methods (or Modified Slope Stability Analysis), and, Working Stress Design Methods. A detailed discussion of the available design methods was provided by the American Society of Civil Engineers (1997), Elias and Juran (1991), CLOUTERRE (1991), and Xanthakos et. al. (1994). During the past decade, several authors have proposed and extended limit equilibrium design methods for a wide variety of site and loading conditions with, and introduced user friendly computer codes.

Limit equilibrium approaches are often used currently in the design of soil nailed structures under both static and seismic loads. Slope stability analysis procedures have been developed to evaluate the global stability of the soil nailed mass and/or the surrounding ground, taking into account the shearing, tensile, or pull-out resistance of the inclusions crossing the potential failure surface. As in traditional slope stability analysis, limit equilibrium conditions are used to search for the most critical failure surface, which can be located either inside or outside the soil nailed retaining structure. The available design procedures involve different assumptions with regard to the shape of the failure surface. British code of practice BS 8006 on strengthened/ reinforced soils and other fills, has suggested a two-part wedge analysis for the evaluation of internal stability of soil nailed structures. However, for more general slopes of varying geometry and multiple soil strata, a method based on circular or non-circular failure surfaces appear to be more appropriate as confirmed by the experimental evidence obtained in this project and elsewhere. Therefore, in this project, two analytical models were developed using limit equilibrium methods, Bishop's simplified method and Janbu's simplified method. This will enable the analysis of both circular and non-circular failure surfaces that are needed under Sri Lankan conditions.

3.1 Analytical Models

3.1.1 Model based on Bishop's simplified method

Bishop's assumption to neglect interslice shear forces was used in the derivation, and the model would be applicable to circular failure surfaces only. All the nails crossing a failure arc of a particular slice, and available within a unit width, are represented by a single nail passing through the center of the failure arc of that particular slice. The final equation for factor of safety is given by;

$$F = \frac{\Sigma\left\{\left[c'\Delta x_i + (W_i + Q_i - u_i\Delta x_i + T_N\sin\alpha)\tan\phi'\varphi\right]\left[1/M_i(\theta)\right]\right\}}{\Sigma\left[(W_i + Q_i)\sin\theta_i - T_N\cos(\theta_i + \alpha)\right]} \quad \text{Eq. (1)}$$

where,

$$M_i(\theta\theta) = \left(\cos\theta_i + \frac{\tan\phi'\varphi\sin\theta_i}{F}\right) \quad \text{Eq. (2)}$$

In this model, only the mobilized tension in the nail is taken into account. Hence,

$$T_N = \text{lesser of}\left[\text{Nail strength, Pullout Resistance}\right] = \text{lesser of}\left[n\frac{\pi\pi d^2}{4}f_y\ ,\ f_b n\pi d\,l(c' + \sigma\sigma\tan\phi')\right] \quad \text{Eq. (3)}$$

Parameters used above are illustrated in Figure 1(a). A complete derivation of this equation is presented by Mettananda et. al. (2001).

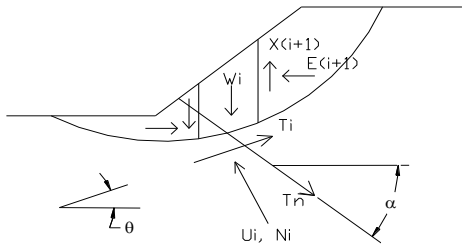

Figure 1(a) : Forces acting on a slice (Bishop's method)

3.1.2 Model based on Janbu's simplified method

Janbu's assumption to neglect interslice shear forces is used in the derivation, and the model can be applied to either circular or non-circular failure surfaces. In order to perform a plane stress analysis, all the nails, applicable to a particular slice over a unit width are represented by a single nail, as done in the Bishop's model. The final equation is given by (Figure 1(b)) ;

$$F_0 = \frac{\Sigma\left\{\left[c'\Delta x_i + (W_i + Q_i + T_N \sin\alpha_i - u_i \Delta x_i)\tan\phi'\varphi\right]\frac{1}{n_{\theta\theta}}\right\}}{\Sigma\left[(W_i + Q_i)\tan\theta_i - T_N \frac{\cos(\alpha + \theta_i)}{\cos\theta_i}\right]} \qquad \text{Eq. (4)}$$

where,

$$n_\theta = \cos\theta_i\left(\cos\theta_i + \frac{\tan\phi'\sin\theta_i}{F}\right) \qquad \text{Eq. (5)}$$

A complete derivation of the formula is presented by Mettananda et.al. (2001).

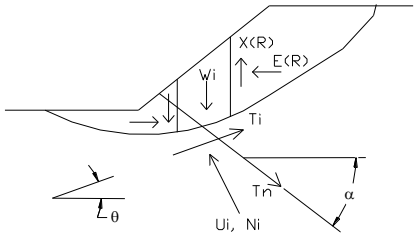

Figure 1(b): Forces acting on a slice (Janbu's method)

After obtaining F_0 from the above equations, the modification factor f_0 is obtained from the charts derived by Janbu, and the final factor of safety is given by,

$F = f_0 F_0$ Eq. (6)

3.2 Development of the spreadsheet and AutoCAD Model

Two spreadsheet programs were developed to perform the calculations based on the above models. Each spreadsheet has three worksheets. They are named as;

(a). Input/ Output Worksheet,

(b). Calculations Worksheet, and ,

(c). Nail Force Worksheet

The input/ output worksheet provides a space for the user to enter input data corresponding to a selected trial failure surface. The nail force worksheet reads data from input worksheet and calculates the resistance provided by nails which pass through that particular slice. The spreadsheet calculates allowable loads due to both tensile strength of the nail and pullout resistance, and selects the minimum value out of them. The calculation worksheet reads data from the other two worksheets, and, performs the calculation to find the factor of safety for the selected trial failure surface. This factor of safety is then transferred to the input/output worksheet, so that the user can directly read it from the input/output worksheet. As such, a general user interacts only with the input/ output worksheet.

To obtain the dimensions of the slices for the trial failure surface considered, another model was developed using AutoCAD. Through this model, once the slope outline is drawn, any number of failure surfaces can be drawn, and the dimensions could be obtained using some fixed slice boundaries within a very short time period (within about 5 minutes).

At the present stage the data on the trial failure surfaces are manually read from the AutoCAD model and entered manually in the input/ output worksheets of the spreadsheet programs.

4.0 Pullout Tests

Pullout resistance tests were conducted on the soil nails prior to the model studies in order to decide on a suitable nail diameter for the model studies, and to find out the bond coefficient available under the test conditions. Tests were done both with a sandy fill and a conventional lateritic fill. The soil compacted to a required density inside a box was expected to represent the natural soil.

The test box had dimensions 0.3m x 0.4m x 0.3m, and the boundary stresses were applied from the top. The effective length of a test nail used was 0.5m. The pullout load was applied through a cable attached to the nail (Figures 2 & 3).

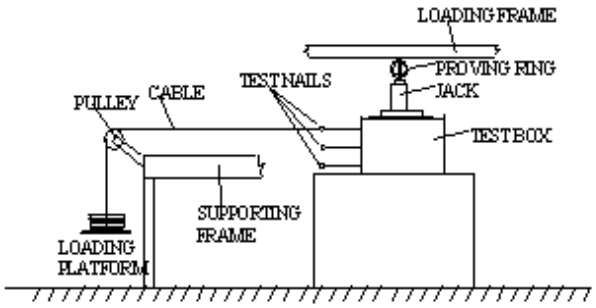

Figure 2 : Test Apparatus

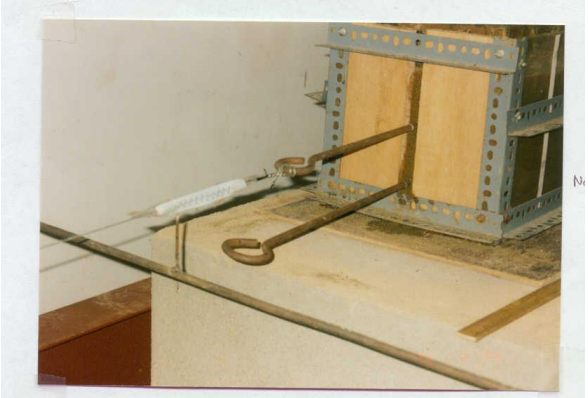

Figure 3: Test Apparatus

Tests on sand were performed for both 10mm and 12mm diameter reinforcing bars. Both plain bars and deformed bars were tested. However, the tests on lateritic soils were limited only to 10mm bars. The vertical surcharges of 20kN/m^2, 40kN/m^2, 60kN/m^2 and 80 kN/m^2 were used in the tests.

The equation used to calculate the pullout resistance is given by,

$$F = f_b * \pi D l (c' + \sigma' \tan\phi) \qquad \text{Eq. (7)}$$

The properties of sand were obtained through direct shear tests, and the friction angle was found to be around 32^0. Lateritic soil, sieved through a 4mm mesh was used, and the properties were established through direct shear tests, sieve analyses, atterberg limit tests and Proctor Compaction tests. Maximum dry density was 1770 kg/m^3, at an optimum moisture content of 16%. The shear strength properties of the as compacted unsaturated material were found to be c' = 20 kN/m^2 and $\phi' = 38.4^0$. The saturated soil had shear strength parameters c'= 20 kN/m^2 and $\phi' = 35.9^0$.

Typical load displacement behaviour obtained is presented in Figures 4. With deformed bars, pullout resistances were expected to be greater than that of the plain bars due to the increased surface roughness. But, the observations were contradictory and none of the tests gave a resistance greater then that for the plain bars. The conclusion that could be arrived regarding this observation was that there had been more disturbances during the driving of deformed bars. Similar observations were made by other researchers as well [Raju, 1996]. Hence, it was decided that the deformed bars are not suitable for the tests.

Also, when compared with the strength of bars, pullout resistances were much smaller (for the selected nail length). Therefore, it was decided that the tensile strength was not critical in selecting a bar size for the model tests. As such, it was decided to conduct the model tests with 10mm bars.

The experimental values obtained for the bond coefficient (f_b) were 1.5 for the sand and 1.6 for the lateritic soil.

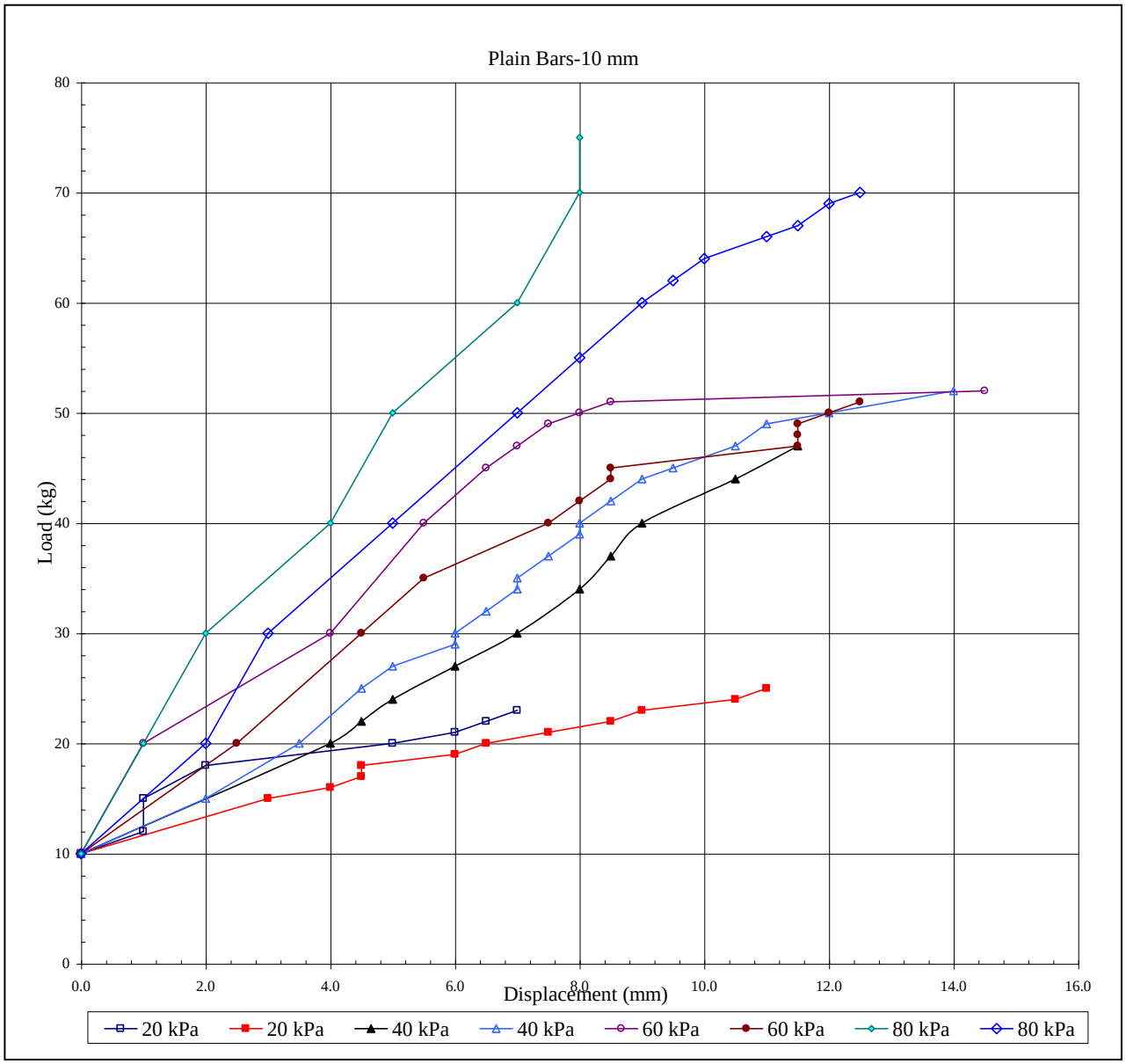

Figure 4 : Load-Displacement Behavior for 10mm Plain Bars in Sand

5.0 Model Studies

Model studies were performed with the objective of identifying the failure loads and failure patterns with and without nails for both sands and lateritic soils, and, verifying the developed analytical programs using the model study data. Although soil nailing is a technique that is used to improve the stability of existing natural slopes, a slope had to be formed by compacting the soil in the laboratory for the model studies.

5.1 Models with Sand Fill

The model was prepared inside a perspex box having dimensions 1.2m x 1.2m x 1m. Sand was placed in 50mm layers and the density was maintained at 1700 kg/m^3. A moisture content of 10% was maintained to facilitate compaction. Alternate layers were coloured in black, in order to visualize the failure surface easily.

The model without nails was made with a slope face at an angle of 33^0 to the horizontal. Flat surface on the top was of plan dimensions 0.4 m x 1.2 m. Load was applied by two jacks, placed on timber planks of area 1.0m x 0.29m. Load increment was 1 kN/m^2, and each load was maintained for 5 minutes. Loading arrangement is shown in Figure 5.

Figure 5 : Loading Set up for Model Tests

First crack appeared on the top surface of the slope at a surcharge of 33 kN/m^2. As the load is increased, more cracks appeared on the slope face and the toe as well, and timber planks started to sink in the sand. Bulging of the toe and outward movement of the slope face was clearly visible. Complete failure of the slope occurred when the surcharge reached 79 kN/m^2 and three circular failure surfaces could be identified at three different sections. All three failure surfaces had originated from the rear edge of the loading area. The geometry of the slope before and after the failure, and the details of the failure surfaces are presented in Figure 6 & Figure 7.

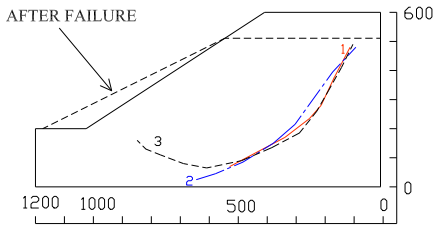

Figure 6 : Failure Surfaces for Models without Nails

Figure 7 : Failure Surface of the Sand Model without Nails

Since the slope could withstand a somewhat higher load and based on the indications that sands can stand at almost vertical slopes for the height of the model, it was decided to increase the inclination of the slope face of the nailed model. Also, the top surface area was increased in order to minimize the end effects, which might exist due to the rear edge of the box.

Hence, the next model had a slope of 45^0, to the horizontal, a top surface of plan area 1.2m x 0.6m, and a toe height of 300 mm. The density, moisture content, layer thickness and the colors of the layers were the same as for the model without nails.

A total of 16 nails, each having a length of 500mm, were inserted in 4 rows. The nails were made of 10mm plain reinforcing bars, and, the nailing arrangement is shown in Figure 8 and Figure 9. A coir mat, placed in position using steel planks, was used as the facing, to avoid local failure.

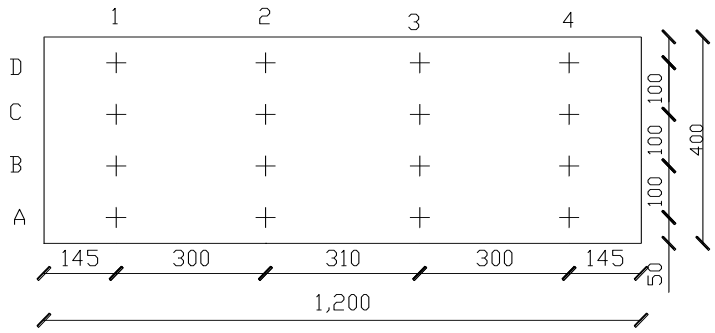

Figure 8 : Nail Arrangement (Front Elevation)
(Dimensions in millimetres)

Figure 9 : Nailing Arrangement

Loading increment was 5 kN/m^2, and each load was maintained for 5 minutes. Small settlements of the loading platform could be observed at a surcharge of 55 kN/m^2. The catastrophic failure was observed at a surcharge of 180 kN/m^2.

Final profile of the slope indicated that significant bulging had taken place, and the details of the slope before and after failure are shown in Figure 10. The failure surface details are presented in Figures 10 and 11. When removing the nails, it could be seen that the nails which were on the top two rows had been bent considerably (see Figure 12). When these bent positions were marked on the original slope profile, they represented a line, very close to the failure surface. From this observation, it could be seen that, once slope started to move, bending stiffness of the nails had also been utilized to stabilize the slope.

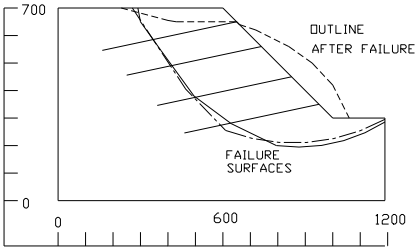

Figure 10 : Failure Surfaces for Models with Nails

Figure 11 : Failure Surface of the Nailed Sand Model

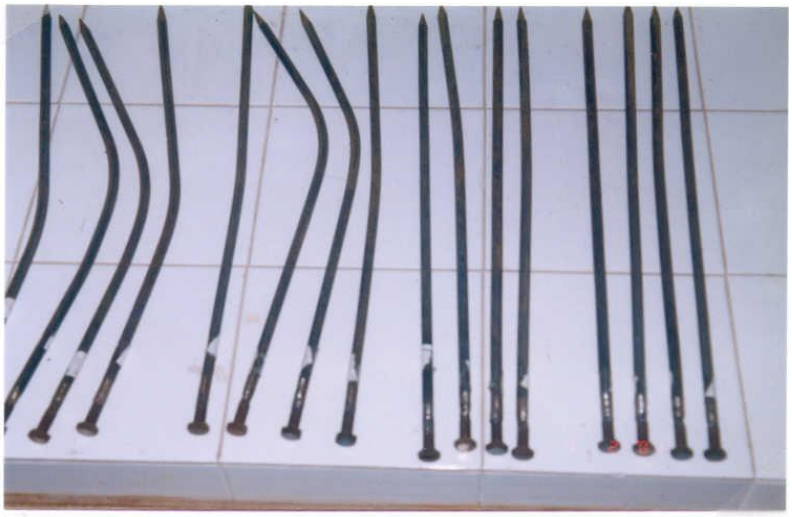

Figure 12 : Bent up Nails Compared with Normal Nails

5.2 Models with Lateritic Fill

Soil was placed in layers having approximate compacted thickness of 50mm. The compaction moisture content was controlled near the optimum of 16%, and the "Proctor Equivalent" energy was applied to obtain the maximum compaction. Compaction was accomplished by applying a calculated number of blows of a hammer, of which, the weight and the height of fall are known.

The slope angle was 60^0 to the horizontal and the area of the top surface was 1.2m x 0.6m. The toe height was reduced to 150mm and the total model height was limited to 525mm due to the practical difficulties in compacting. Initially, the model was prepared in steps, and, the slope face was trimmed subsequently to get a smooth inclined surface of 60^0 inclination. This was done in order to facilitate uniform compaction even near the slope face. After the compaction, the model was wetted continuously, by pooling water on the top surface, to make it saturated. Load was applied in increments of 10 kN/m^2, and each load was maintained for 5 minutes.

When the model was loaded, settlement of the top surface became visible when the surcharge reached 80 kN/m^2. When the surcharge is 100 kN/m^2, some bulging and cracking could be seen on the middle part of the slope face. At 135 kN/m^2, cracks near the toe of the slope appeared. Timber planks started to sink at 160 kN/m^2, and the rate of deformations at the toe became high after 175 kN/m^2. The model was loaded up to 480 kN/m^2. Finally, a shallow local crack could be observed along the slope. As the crack had initiated from the front end of the loading platform, it could not be back analyzed using the models developed. Although, the model could withstand further loading, greater loadings could not be applied due to the limitations of the proving rings. However based on the observed deformations, the slope was deemed to have failed.

Actual moisture content of the model at the time of testing was about 18.9%. Bulk density was 1996 kg/m^3, and the dry density was around 1679 kg/m^3. The direct shear tests conducted on samples taken from the model revealed that the actual shear strength parameters were c'= 20.9 kN/m^2 and $\phi' = 35.9^0$. The degree of saturation was observed to be 86.6 %.

Since a catastrophic failure of the expected form could not be observed for the model without nails, where soil was compacted to Proctor Energy, it was decided to use a model with a lesser compaction effort. Also, it was anticipated that lesser compaction would help the subsequent saturation. Therefore a lesser energy (35% of Proctor Energy) was applied to compact the next model. This was expected to represent a less competent natural soil deposit.

Dimensions of the model were exactly the same as for the earlier model. A total number of 16 nails was installed, with the four bottom nails having a lesser length of 400mm. It was done with the objective of preventing them touching the base. Nail angle was 17^0 to the horizontal, but same facing type as earlier was used here as well. After constructing the model, it was wetted constantly to achieve saturation. At the time of loading the model had been well saturated, with water been squeezed out around the model. The degree of saturation was observed to be 96%. Loading was done in the usual manner.

Small settlements and diagonal cracks on the top surface started to appear after 140 kN/m^2. After 160 kN/m^2, timber planks started to sink. At a load of 240 kN/m^2, some bulging and cracking could be seen on the slope face as well. After 330 kN/m^2, cracks on the side face also appeared. Loading was continued up to a surcharge of 500 kN/m^2. Further loading could not be performed due to the limitations of the proving rings. At this load, a considerable shifting of the slope face could be observed. This shift was about 1 cm at 400 kN/m^2, but started to move faster after 430 kN/m^2, and the final value was about 4.5 cm. Settlement of the load at this moment was 35mm which was higher compared with the earlier model. However, in contrast to the earlier observations, no failure surface could be identified, when the model was excavated. However, the nails had been bent here as well.

6.0 Back Analysis of Results

6.1 Models with sandy fill

The failure surface of the model without nails was back analyzed using the analytical model developed based on Bishop's method. The results are presented in tables 1 and 2. Table 1 presents the factor of safety values obtained at the failure surcharge of 79 kN/m^2. Table 2 presents the surcharge corresponding to a factor of safety of unity. The analyses were performed with a range of shear strength parameters selected based on the results of the direct shear tests. A small apparent cohesion, which could be there when the sand is in a wet, partially saturated condition was used in some of the analyses.

Failure surface 2 touched the base, as well as the support provided in front of the toe. Effects at these supports could not be quantified in the analysis easily. Hence, more emphasis was placed upon the failure surfaces 1 and 3 (Figure 6).

If only the failure surfaces 1 and 3 are considered in the analysis, it could be observed that more closer values for the failure load is given by the shear strength parameters c'=2 kN/m^2 and $\phi'=32^0$. Hence, the set of parameters c'=2 kN/m^2 and $\phi'=32^0$ appear to be a reasonable average value. This observation clearly gives an evidence for the presence of an apparent cohesion in the wet sand. Similar observation had been made by some other researchers as well.

Back analysis of the nailed model was done based on the observed non-circular failure surface using the model developed based on Janbu's method. The results obtained are presented in Tables 3 and 4. The same failure surface was analyzed for the case without nails, and those results are also tabulated. The analyses were performed for the same shear strength parameters that were used for the earlier model.

When back analysis was performed with parameters c'=2 kN/m^2 and ϕ'=32^0, the failure load would have increased to 100 kN/m^2. These results were based on a f_b value of 2.0 for the nails. However, the actual failure load of the model was very much greater than this value. Since the nails had been bent considerably, this difference could be attributed to the mobilization of bending stiffness of the nails.

Table 1: Results of the Back Analysis (Sand Model without nails) – Factors of Safety at the failure load (79 kPa)

Slip Surface	FOS For c'=0, ϕ'=32^0	FOS For c'=1 kPa, ϕ'=32^0	FOS For c'=2 kPa, ϕ'=32^0	FOS For c'=0, ϕ'=34^0	FOS For c'=2 kPa, ϕ'=34^0
3	0.86	0.94	1.02	0.93	1.08
1	0.80	0.87	0.93	0.86	1.00
2	1.03	1.22	1.39	1.11	1.48

Table 2: Results of the Back Analysis (Sand Model without nails) - Value of surcharge to give FOS = 1

Slip Surface	q (kPa) For c'=0, ϕ'=32^0	q (kPa) For c'=1 kPa, ϕ'=32^0	q (kPa) For c'=2 kPa, ϕ'=32^0	q (kPa) For c'=0, ϕ'=34^0	q (kPa) For c'=2 kPa, ϕ'=34^0
3	40	60	85	50	110
1	30	50	60	40	79
2	85	150	210	130	320

Table 3: Results of the Back Analysis (Sand Model with nails) – Factors of Safety at the failure load (180 kPa)

Slip Surface	FOS For c'=0, ϕ'=32^0	FOS For c'=1 kPa, ϕ'=32^0	FOS For c'=2 kPa, ϕ'=32^0	FOS For c'=0, ϕ'=34^0	FOS For c'=2 kPa, ϕ'=34^0
With Nails	0.84	0.87	0.91	0.92	1.00
Without Nails	0.57	0.60	0.63	0.62	0.67

Table 4: Results of the Back Analysis (Sand Model with nails) - Value of surcharge to give FOS = 1

Slip Surface	q (kPa) For c'=0, ϕ'=32^0	q (kPa) For c'=1 kPa, ϕ'=32^0	q (kPa) For c'=2 kPa, ϕ'=32^0	q (kPa) For c'=0, ϕ'=34^0	q (kPa) For c'=2 kPa, ϕ'=34^0
With Nails	20	50	100	50	180
Without Nails	4	15	25	5	30

6.2 Models with lateritic fill

The model without nails did not give a failure surface that could be analyzed using the developed programs. However, it could be clearly observed that the model with nails could resist the shallow failure surface even though the soil and had a higher degree of saturation had been subjected to a lesser compactive effort.

7.0 Applications to some Real Slope Problems in Sri Lanka

Sri Lanka has been experiencing a spate of landslides over extensive areas of its central and southwestern regions since the early eighties. Some of the major slides taken place are Watawala slide, Naketiya slide, Hela-Uda slide (Ratnapura), Beragala slide and Haldummulla slide.

Almost all the landslide events reported had taken place after heavy rain. It indicates that the slopes that are stable in dry weather have become unstable, once high pore water pressures are developed. Also, reports show that most of the landslides had shown prior indications through the accumulated displacements that have taken place over a long period of time

(sometimes over 50 to 100 years). These deformations would have reduced the peak shear strength parameters towards the residual values, eventually lowering the factor of safety of the slope. Since there is a high probability of having a lowered factors of safety, it is preferable to have some external support systems to stabilize those slopes. Soil Nailing would be an appropriate method to provide this support.

Major difficulty faced here was in obtaining of past records. Although some reports could be found regarding the landslides [Rajaratnam and Bandari (1994), Ministry of Forestry and Environment (1997)], there were no direct records about the failure surfaces or the soil strength parameters. In the absence of direct records, the following analysis is based on best possible information that could be derived from the data available. Hence, the results presented here are approximate.

7.1 Watawala Landslide

This is one of the most extensively studied landslides in Sri Lanka. The slide boundaries had been established through a systematic program of field mapping, site investigation, slope instrumentation and monitoring (Figure 15). Piezometric levels are known, and residual shear strength parameters were determined to be c'=0 and $\phi_r = 16^0$.

When the failure surfaces were analysed, it could be seen that, most of the time, the failure surface is more than 20m below. Hence, if it is to be stabilized only using soil nailing, that would require long nails in the range of 30-35m. But, the maximum nail length reported in literature is 23m. As such, soil nailing cannot be used as the sole method of improving the stability. Soil nailing could be used at shallow areas of the instability along with surface and subsurface drainage to reduce the development of excess pore water pressure.

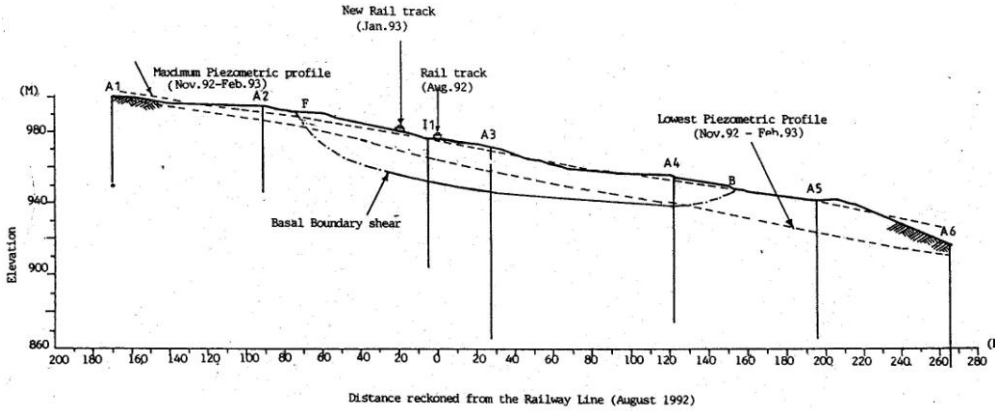

Figure 13 : Failure Surface of Watawala Landslide

7.2 Beragala Earthslip

Consideration was given only to the shallow failure mass that was in between Haputale road and Wellawaya road. In the absence of the soil strength parameters, a reasonable estimate of c=15 kN/m^2 and $\phi'=32^0$ was used for the analysis. The bulk density used was 18 kN/m^3. Highest level of the water table was assumed to be along the slope face during wet weather and the lowest level of the water table is assumed to be below the failure surface.

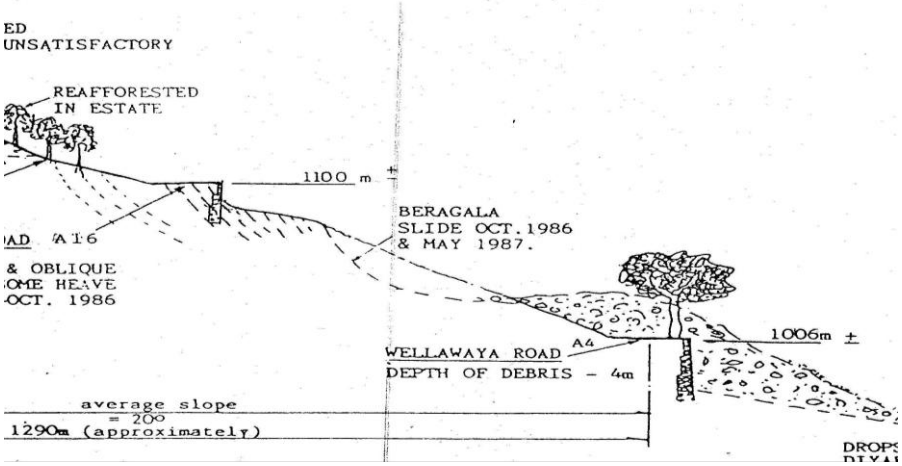

Figure 14 : Beragala Earthslip

The back analysis showed a factor of safety of 1.10 in dry weather condition. It, decreases to 0.61, once the pore pressures developed due to the high water table. Designed nail arrangement consisted of 25mm diameter nails of lengths 18m and 12m, and is presented in Figure 16. The nails were on a grid of 1m x 1m. When this nailed slope was back analyzed, the factor of safety under wet condition improved to 1.56. When the same nails were arranged on a grid of 1.2m x 1.2m, the improved factor of safety was 1.13, under the high water table.

8.0 Conclusion

The observed failure surfaces can be accurately modelled by circular and non-circular failure surfaces. This satisfies the development of analytical models based on the Bishop's and Janbu's methods.

From the sensitivity analysis, it was shown that, soil nailing can improve the factor of safety of a slope under both dry and wet conditions. Model studies were done to verify these observations. Due to the practical limitations, the tests were limited to driven nails only. Pullout resistance tests showed that the pullout resistance provided by the driven nails could be greatly reduced by the disturbances caused during driving. Hence, special care has to be taken during driving of nails. From the results of the pull out tests, a suitable nail type was selected for the model studies and the bond coefficient was calculated.

The results of the sand models showed that the nails can improve the stability of the slopes by providing a permissible load increase of over 400%. However, due to the practical limitations in applying higher loads, which needed to fail lateritic models, such comparison could not be obtained using the lateritic models. However, from indirect evidences, it was convinced that an improvement in stability could be achieved in such soils also.

In the study of actual case histories, it was observed that most of the limited data available corresponded to deep seated failures. Hence, they could not be stabilized using soil nailing alone. The most economical solution will be to use nails in combination with proper drainage. However, results of the Beragala slide showed that shallow failures could be stabilized satisfactorily using nailing.

9.0 References

American Society of Civil Engineers (1997), “Ground Improvement, Ground Reinforcement, Ground Treatment – Developments 1987-1997”, Geotechnical Special Publication No. 69, Virginia.

Bruce, D.A. and Jewel, R.A. (1986), "Soil Nailing: Application and Practice-part 1", Ground Engineering, November, 10-15.

Bruce, D.A. and Jewel, R.A. (1987), "Soil Nailing: Application and Practice-part 2", Ground Engineering, January, 21-34.

CLOUTERRE (1991), "The Technique Used For Soil Nailed Structures : Description And Developments",www.terrasol.com.

Elias, V. and Juran, I. (1991), "Soil Nailing for Stabilization of Highway Slopes and Excavations", United States Federal Highway Administration, Publication No. FHWA-RD-89-193, June.

Hewitt P. and Haustorfer I. (2000),"Hitting the Highway", Ground Engineering, February, P.28.

Mettananda, D.C.A., Premarathna, B.D.H. and Priyantha, H.M.S. (2001),”The use of soil nailing technique in stabilization of slopes”, Final Year Project Report, University of Moratuwa.

Ministry of Forestry and Environment, Sri Lanka (1997), "The Report on Landslides in Badulla District During 1997".

Mitchell J.K. and Villet C.B. (1987),"Reinforcement of Earth Slopes and Embankments", NCHRP Report 290, Transport Research Board, Washington, 258-312.

Ortigo J. A. R., Palmeira E. M. and Zirlis A.C. (1995) , “Experience with Soil Nailing in Brazil:1970-1994”, Proceedings of the Institution of Civil Engineers (London), Geotechnical Engineering, April 1995, pp 93-106

Rajaratnam, K. and Bhandari, R.K., (1994),"Back Analysis of the Watawala Earthslide in Terms of Effective Stress", Proceedings of the National Symposium on Landslides in Sri Lanka, National Building Research Organization, Sri Lanka, 119-127.

Raju, G.V.R. (1996), "Behavior of Nailed Soil Retaining Structures", PhD Thesis, Nanyang Technological University, Singapore.

Xanthakos P.P., Abramson L.W. and Bruce D.A. (1994), "Ground Control and Improvement" , John Wiley & Sons Inc., New York, 331-405.

Notations

F - Factor of safety
c' - Cohesion
Δx_i - Width of 'i' th slice
W_i - Weight of 'i' th slice
Q_i - Surcharge applied on 'i' th slice
u_i - Pore water pressure acting on 'i' th slice
T_N - Mobilized force in nails (applicable to 'i' th slice)
α - Nail inclination to the horizontal
Φ' - Angle of internal friction
$M_i(\theta)$, n_θ - Modification factor applicable to 'i' th slice
n - Number of nails
d - Diameter of nails
f_y - Yield strength of steel
f_b - Bond coefficient
l - Effective length of nails
σ' - Average circumferential stress around nails = ½ ($\sigma_v'+\sigma_H'$)
σ_v', σ_H' - Vertical and horizontal effective stresses
F_0 - Initial factor of safety from Janbu's method
f_0 - Modification factor obtained from charts developed by Janbu

Cavity Expansion Analysis for Sand Compaction Piles

Udeni P.Nawagamuwa
Doctoral Student, Department of Civil Engineering
Yokohama National University, Japan

(Former Research Student of Geomechanics Group, GTE Program)
School of Civil Engineering, Asian Institute of Technology
Thailand

ABSTRACT
Strength parameters of a sand compaction pile are normally checked by standard penetration test (SPT). Empirical equations, which are derived from numerous data obtained from uniform sand, are adopted for evaluating internal friction angle (ϕ') of the sand pile. However, constraint conditions of a sand pile in a clay formation improved with sand column piles (SCPs) are considered to be very different from that in a uniform sand. Due to simplicity, speed, continuous profiling and amenability to theoretical modeling, cone penetration tests (CPT) can be used to evaluate ϕ' for SCP. The most important data from the SCPs is the cone penetration resistance.

A theory, based on cavity expansion, was developed for computing the cone penetration resistance of sand. The sand was modeled as an elastic-plastic material with a plastic zone and an elastic zone, and the spring action generated by the surrounding clay to transfer the confining stresses to the SCP was considered. This theory can be used for analysis of calibration chamber tests, as it takes full account of the SCP dimensions and boundary conditions. In addition, a parametric study was done to observe the behavior of SCP for different input parameters.

The agreement between Vesic theory and the theory developed using cavity expansion for infinite soil mass was 100%. The developed theory yields a good linear relationship between the ultimate cavity pressure and the internal friction angle.

1.0 Introduction

From an engineering standpoint, the shortage of suitable land for construction is becoming more serious. In order to utilize soft-ground areas previously deemed incompetent, many ground improvement techniques have been proposed. Soft ground improvement is applicable mainly in lowland environments such as coastal areas in South East Asia, Japan and the U.S.A. This is also applicable in similar conditions and environments like the peat deposits in Colombo, Sri Lanka. One of the best ways for soft ground improvement is the use of granular piles or sand compaction pile (SCP).

The method of SCP improvement can be classified into two types in terms of a replacement area ratio: a high replacement SCP with the replacement ratio of 70-80% and a low replacement SCP with ratio about 25%-50%. As a method for evaluating the effect of high replacement SCP, the strength of the improved ground is determined based on the volume of sand piles driven into the ground and their strength, which is evaluated using a standard penetration test (SPT N-value). For the case of low replacement SCP, they are expected not only to bear the load placed on the ground, but also to drain pore water in soft soil to enhance consolidation of the soil. Therefore, the ground improved by low replacement SCP should be evaluated as a composite ground consisting of sand piles and soft soil. The strength of composite ground increases with time when low replacement SCPs are applied.

Strength parameters of a sand compaction pile are normally checked using SPT. Empirical equations, which are derived from numerous data obtained from uniform sand, are adopted for evaluating the ϕ' value of a sand pile. However, constraint conditions of a sand pile in clay improved with SCP, as shown in Figure 1(b), are considered to be very different from that in the uniform sand as shown in Figure 1(a).

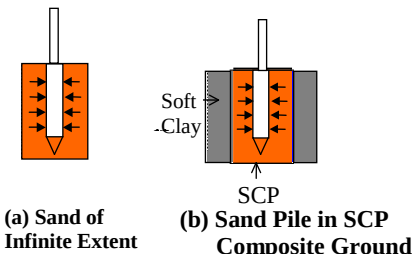

Figure 1

The angle of friction in sand, ϕ_s is normally back calculated using empirical equations like the following:

$$\phi_s = 20 + (12N)^{1/2} \quad \text{or } \phi_s = (18N_{70})^{1/2} + 15$$

where N= SPT number and N_{70} = SPT number for energy ratio 70% (Dunham,1954). However, this method may underestimate the ϕ_s value in SCP improved ground. In addition, the confining pressure from the surrounding composite ground, σ_h depends on the replacement ratio. The higher the area replacement ratio (a_s) the higher the σ_h, where a_s is defined as the ratio between

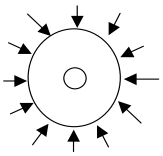

Figure 2 : Confining Pressure from the Surrounding

the horizontal area of SCP to total area.

Cavity expansion theory for finite soil mass and Vesic equations for infinite soil mass are widely used in the analysis of this type of situations using cone penetration resistance when a cone is penetrated into the soil.

2.0 Cavity Expansion Theory

The problem of expansion of cavities in an ideal soil mass has connections with bearing capacity of deep foundations, interpretation of pressure meter tests, cratering by explosives and breakout resistance of anchors.

Cavity expansion analysis consists of determining the cavity pressure required to expand a cavity in a material medium by a certain amount. There are two types of cavity expansion problems. In the first, a cavity exists initially in the soil and the pressure in the cavity is in equilibrium with the stresses in the surrounding soil and an ever-increasing pressure is required to continue expanding the cavity. In the second, there is initially no cavity in the soil mass and any cavity expansion will start from an initial cavity radius equal to zero (Salgado et.al.1997).

The cone penetration resistance is a function of limit cylindrical cavity pressure. Soil behaves as a rigid plastic, incompressible solid in a plastic region surrounding the cavity and as a linearly deformable solid beyond the region.

A spherical cavity of initial radius R_i expanded by a uniformly distributed internal pressure P is considered (Vesic, 1972). If this pressure is increased, a spherical zone around the cavity will pass into the state of plastic equilibrium. This plastic zone will expand until the pressure reaches an ultimate value P_u. At this moment the cavity will have a radius, R_u (Figure 3).

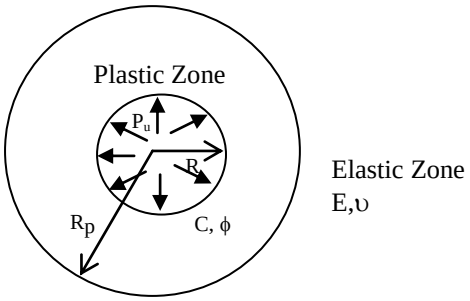

Figure 3 : Cavity expansion generates a plastic zone

To determine P_u and R_p, it is assumed that the soil in the plastic zone behaves as a compressible plastic solid defined by c, ϕ and volumetric strain Δ. Beyond the plastic zone, the soil is assumed to behave as a linearly deformable, isotropic solid defined by E and υ.

It was shown by Vesic (1972) that the principal parameters affecting ultimate pressure are the initial effective ground stress, strength and volume change characteristics of the soil as well as the rigidity index of the soil defined as the ratio of its shear modulus to its initial shear strength. The radius of the plastic zone depends primarily on the rigidity index of the soil.

3.0 Case Studies for Cavity Expansion Analysis (Chen and Juang, 1996)

3.1 Hunter's Point, California Site

The minor difference in the predicted ϕ' values obtained by the Vesic method and the correlation in this case suggests that a reliable estimate of ϕ' of sands from CPT data may be made by the former method with a known K_0. It also suggests that K_0 may be back calculated from the cavity expansion theory (Vesic's method), if ϕ' is known.

3.2 Texas A&M University Site

The cavity expansion theory, with an empirical correlation established in this study for determining the volumetric strain based on CPT data, may reliably predict ϕ' of sands from CPT data, if K_0 is given. On the other hand, if ϕ' is known, the theory may reliably predict K_0 of sands from CPT data.

3.3 Northwestern University Site

The procedure for determining ϕ' of an over-consolidated (OC) sand using Vesic's method is essentially the same as in the case of normally-consolidated (NC) sand, provided that the equivalent $q_{c(NC)}$ and $K_{0(NC)}$ can be obtained. This case study shows that ϕ' of an OC sand can be reliably determined by Vesic's cavity expansion theory using CPT data, if the OCR (Over Consolidation Ratio) is given.

$$\frac{q_{c(OC)}}{q_{c(NC)}} = 1 + 0.75\left(\frac{K_{0(OC)}}{K_{0(NC)}} - 1\right) \qquad \text{Eq. (1)}$$

where $\frac{K_{0(OC)}}{K_{0(NC)}} = (OCR)^{\beta}$ and β = an empirical constant.

However the effect of overconsolidation on CPT measurement is not well understood at present, and thus, more studies are needed to further validate the presented procedure.

4.0 Theoretical Study with Vesic Theory and Cavity Expansion Theory

It is assumed that the soil in the plastic zone behaves as a compressible plastic solid defined by Coulomb–Mohr shear strength parameters C and ϕ, as well as by an average volumetric strain Δ, which can be determined from known states of stress in the plastic zone and volume change - stress relationships. Beyond the plastic zone, the soil is assumed to behave as a linearly deformable, isotropic solid defined by modulus of deformation, E, and Poisson's ratio (υ).

4.1 Vesic Theory for Infinite Soil Mass

General solutions of the problems of expansion of spherical and cylindrical cavities in an ideal soil, possessing both cohesion and friction in the Coulomb – Mohr sense are presented here.

4.1.1 Problem of Spherical Cavity

Definition of the Variables:
ϕ – Angle of Internal Friction
E – Modulus of Elasticity
Δ – Volumetric strain
υ – Poisson's ratio
C – cohesion

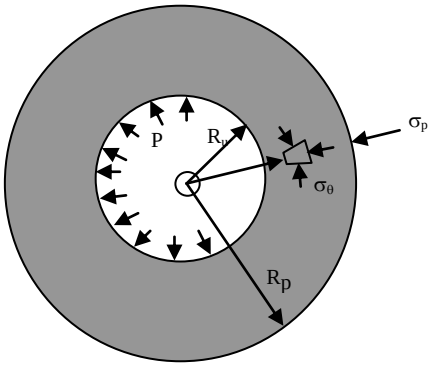

Figure 4. Expansion of Cavity for Infinite Soil Mass (Vesic, 1972)

The ultimate cavity pressure can be found as,

$$P_u = C.\cot\phi.F_c + q.F_q \qquad \text{Eq. (2)}$$

where

$$F_q = \frac{3(1+\sin\phi)}{3-\sin\phi}[I_{rr}]^{\frac{4\sin\phi}{3(1+\sin\phi)}}$$

$$F_c = F_q - 1$$

$$I_r = \frac{G}{S} = \frac{E}{2(1+\upsilon)(c+q.\tan\phi)}$$

$$I_{rr} = \frac{I_r}{1+\Delta I_r}$$

where, I_r = Rigidity Index

Δ =Volumetric Strain

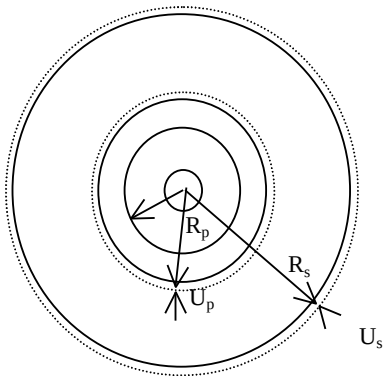

Figure 5 : Expansion of Cavity in Finite Soil Mass

4.1.2 Problem of Cylindrical Cavity

This problem is completely analogous to the previous one, with the difference that it is axially symmetrical instead of spherically symmetrical.

The ultimate cavity pressure can be found as,

$$P_u = CF'_c + qF'_q \qquad \text{Eq. (3)}$$

where

$$F'_q = (1+\sin\phi)[I'_{rr}\sec\phi]^{\frac{\sin\phi}{1+\sin\phi}}$$

$$F'_c = (F'_q - 1)\cot\phi$$

and I'_{rr} = the reduced rigidity index

$$I'_{rr} = \frac{I_r}{1+\Delta I_r \sec\phi}$$

4.2 Cavity Expansion Theory for Finite Soil Mass

A theory, based on cavity expansion, is developed for computing the cone penetration resistance and ultimate cavity pressure of sand with different internal friction angles. Later it is extended for a parametric study for 2D and 3D cases.

4.2.1 Problem of Spherical Cavity

Spherical cavity expansion in sand with finite boundaries

Definition of the Variables

ϕ - Angle of Internal Friction
R_s - Radius of the SCP
R_c - Radius of the Cone
K_h - Coefficient of the sub grade reaction
σ_p - Stress at the elastic-plastic boundary
Δ - Volumetric strain
υ - Poisson's ratio
U_p- Displacement at the elastic-plastic boundary
U_s -Displacement in the SCP

From the Equation of Equilibrium,

$$\frac{\partial \sigma_r}{\partial r} + 2\frac{\sigma_r - \sigma_\theta}{r} = 0 \qquad \text{Eq. (4)}$$

After Timoshenko and Goodier (1951) and Yu (200) the solution of Eq. (4) is :
Solution for equation (4);

$$\sigma_r = \frac{A}{r^3} + 2A_1$$

$$\sigma_\theta = -\frac{A}{2r^3} + 2A_1$$

when $(\sigma_r)_{r=R_p} = (\sigma_p - q)$ and $(\sigma_r)_{r=R_S} = u_s k_h$:

$$A = \frac{R_s{}^3 R_p{}^3 (\sigma_p - q - u_s k_h)}{(R_s{}^3 - R_p{}^3)}$$

$$2A_1 = -\frac{R_s^3(\sigma_p - q) - u_s k_h R_s^3}{\left(R_s^3 - R_p^3\right)}$$

and then the solution becomes,

$$\sigma_r = \frac{R_s{}^3 R_p{}^3 (\sigma_p - q - u_s k_h)}{(R_s{}^3 - R_p{}^3)}\frac{1}{r^3} - \frac{R_p{}^3 (\sigma_p - q) - u_s k_h R_s{}^3}{(R_s{}^3 - R_p{}^3)} \qquad \text{Eq. (5)}$$

$$\sigma_\theta = -\frac{R_s{}^3 R_p{}^3 (\sigma_p - q - u_s k_h)}{(R_s{}^3 - R_p{}^3)}\frac{1}{2r^3} - \frac{R_p{}^3 (\sigma_p - q) - u_s k_h R_s{}^3}{(R_s{}^3 - R_p{}^3)} \qquad \text{Eq. (6)}$$

Using the condition of rupture (Mohr circle), $(\sigma_r - \sigma_\theta) = (\sigma_r + \sigma_\theta)\sin\phi + 2C.\cos\phi$ Eq. (7)

Thus, $\frac{\sigma_\theta + C.\cot\phi}{\sigma_r + C.\cot\phi} = \frac{1 - \sin\phi}{1 + \sin\phi}$ Eq. (8)

Change of volume of the cavity = change of volume of the elastic zone + change of volume of the plastic zone + change of volume of SCP

Change of volume of the cavity = $R^3{}_u - R^3{}_i$
Change of volume (decrease) of the elastic zone = $(R^3{}_s - R^3{}_p) - \{(R_s + u_s)^3 - (R_p + u_p)^3\}$
Change of volume of the plastic zone = $(R^3{}_p - R^3{}_u)\Delta$
Change of volume of SCP = $(R_s + u_s)^3 - R^3{}_s$

Thus, $R^3{}_u - R^3{}_i = [(R^3{}_s - R^3{}_p) - \{(R_s + u_s)^3 - (R_p + u_p)^3\}] + (R^3{}_p - R^3{}_u)\Delta + [(R_s + u_s)^3 - R^3{}_s]$

Neglecting higher order terms of u_p and u_s and assuming $R_i = 0$,

$1 + \Delta = \frac{3R^2{}_p}{R^3{}_u}u_p + \frac{R^3{}_p}{R^3{}_u}\Delta$, and $[\frac{R_u}{R_p}]^3(1+\Delta) = \frac{3u_p}{R_p} + \Delta$

$\{[\frac{R_u}{R_p}]\ (1+\Delta)^{\frac{1}{3}}\}^3 = \frac{3u_p}{R_p} + \Delta$, but $(1+\Delta)^{\frac{1}{3}} \approx 1$, so $[\frac{R_u}{R_p}]^3 = \frac{3u_p}{R_p} + \Delta$

as, $u_p = \frac{R_p}{(R_s{}^3 - R_p{}^3)E}[(1-2\upsilon)\{(\sigma_p - q)R_p{}^3 - u_s k_h R_s{}^3\} + \frac{(1+\upsilon)}{2}(\sigma_p - q - u_s k_h)R_s{}^3]$ Eq. (9)

Proof of (9):

$\varepsilon_r = -\frac{du}{dr}$ and $\varepsilon_\theta = -\frac{u}{r}$ where $u = -r.\varepsilon_\theta$

For elastic materials.

$\varepsilon_r = \frac{1}{E}[\sigma_r - 2\upsilon\sigma_\theta]$, $\varepsilon_\theta = \frac{1}{E}[-\upsilon\sigma_r + (1-\upsilon)\sigma_\theta]$ and $u = -r.\varepsilon_\theta$

$$u = -\frac{r}{E}\{-\upsilon[2C + \frac{A}{r^3}] + (1-\upsilon)[2C - \frac{A}{2r^3}]\}$$

$$u = -\frac{r}{E}\{2C(1-2\upsilon) - \frac{A}{r^3}\frac{(1+\upsilon)}{2}\}$$

$$u = \frac{r}{E}\{(1-2\upsilon)[\frac{R_p{}^3(\sigma_p - q) - u_s k_h R_s{}^3}{(R_s{}^3 - R_p{}^3)}] + \frac{1}{r^3}\frac{(1+\upsilon)}{2}[\frac{R_s{}^3 R_p{}^3(\sigma_p - q - u_s k_h)}{(R_s{}^3 - R_p{}^3)}]\}$$

when $r = R_p$ and $u = u_p$ then,

$$u_p = \frac{R_p}{(R_s{}^3 - R_p{}^3)E}[(1-2\upsilon)\{(\sigma_p - q)R_p{}^3 - u_s k_h R_s{}^3\} + \frac{(1+\upsilon)}{2}(\sigma_p - q - u_s k_h)R_s{}^3]$$

and when $r = R_s$ and $u = u_s$ then,

$$u_s = \frac{R_s}{(R_s{}^3 - R_p{}^3)E}[(1-2\upsilon)\{(\sigma_p - q)R_p{}^3 - u_s k_h R_s{}^3\} + \frac{1+\upsilon}{2}(\sigma_p - q - u_s k_h)R_p{}^3] \quad \text{Eq. (10)}$$

Therefore,

$$[\frac{R_u}{R_p}]^3 = \frac{3}{(R_s{}^3 - R_p{}^3)E}[(1-2\upsilon)\{(\sigma_p - q)R_p{}^3 - u_s k_h R_s{}^3\} + \frac{1+\upsilon}{2}(\sigma_p - q - u_s k_h)R_s{}^3] + \Delta$$

Using (10),

$$u_s[1 + \frac{R_s}{(R_s{}^3 - R_p{}^3)E}\{(1-2\upsilon)k_h R_s{}^3 + \frac{(1+\upsilon)}{2}k_h R_p{}^3\} = \frac{R_s}{(R_s{}^2 - R_p{}^2)E}[(1-2\upsilon)(\sigma_p - q)R_p{}^3 + \frac{(1+\upsilon)}{2}(\sigma_p - q)R_p{}^3]$$

$$u_s = \frac{\frac{3}{2}(1-\upsilon)(\sigma_p - q)R_p^3}{K_h[(1-2\upsilon)R_s^3 + \left(\frac{1+\upsilon}{2}\right)R_p^3] + \frac{E(R_s^3 - R_p^3)}{R_s}} \quad \text{Eq. (11)}$$

Considering the compatibility condition at elastic-plastic boundary;

$$\frac{\sigma_r + 2\sigma_\theta}{3} = q - \frac{(\sigma_p - q)R^3{}_p - u_s k_h R^3{}_s}{(R^3{}_s - R^3{}_p)} \quad \text{Eq. (12)}$$

$$(\sigma_r - \sigma_\theta) = (\sigma_r + \sigma_\theta)\sin\phi + 2c.\cos\phi$$

then, $\sigma_\theta = \frac{\sigma_r(1-\sin\phi) - 2C\cos\phi}{1+\sin\phi}$

so, $\frac{\sigma_r + \sigma_\theta}{3} = \frac{\sigma_r + 2\frac{\sigma_r(1-\sin\phi) - 2C\cos\phi}{1+\sin\phi}}{3}$

by solving above equation with Eq.(12),

$$q - \frac{R_p{}^2(\sigma_p - q) - u_s k_h R_s{}^2}{(R_s{}^2 - R_p{}^2)} = \frac{\sigma_r(3\sin\phi - 1) - 4C\cos\phi}{3(1+\sin\phi)}$$

and at the boundary $\sigma_r = \sigma_p$

$$\sigma_p(R_s^3 - R_p^3)(3\sin\phi - 1) - 4C.\cos\phi(R_s^3 - R_p^3) = 3[(R_s^3 - R_p^3)q - (\sigma_p - q)R_p^3 + U_s k_h R_s^3](1+\sin\phi)$$

$$\sigma_p[R_s^3(3\sin\phi - 1) + 4R_p^3] = 4C.\cos\phi(R_s^3 - R_p^3) + 3R_s^3(1+\sin\phi)q + 3(1+\sin\phi)U_s k_h R_s^3 \quad \text{Eq. (13)}$$

By using equations (5), (6), (7) ,(11), (12) and (13) it can be found that;

$$\sigma_p = \frac{4C.\cos\phi(R_s^{\ 3} - R_p^{\ 3}) + 3R_s^{\ 3}(1+\sin\phi)q - \dfrac{\frac{9}{2}(1-\upsilon)qR_p^{\ 3}k_h(1+\sin\phi)}{k_h\{(1-2\upsilon)R_s^{\ 3} + \frac{(1+\upsilon)}{2}R_p^{\ 3}\} + \dfrac{E(R_s^{\ 3} - R_p^{\ 3})}{R_s}}}{\{R_s^{\ 3}(3\sin\phi - 1) + 4R_p^{\ 3} - \dfrac{\frac{9}{2}(1-\upsilon)R_p^{\ 3}k_h(1+\sin\phi)}{k_h\{(1-2\upsilon)R_s^{\ 3} + \frac{(1+\upsilon)}{2}R_p^{\ 3}\} + \dfrac{E(R_s^{\ 3} - R_p^{\ 3})}{R_s}}\}} \quad \text{Eq. (14)}$$

For 3D case ultimate cavity pressure can be computed using the following expression

$\sigma_p = (P_u + C\cot\phi)\left(\frac{R_u}{R_p}\right)^{\frac{4\sin\phi}{1+\sin\phi}} - C.\cot\phi$ where P_u is the ultimate cavity pressure.

4.2.2 Problem of Cylindrical Cavity

Cylindrical cavity expansion in sand with finite boundaries

From the Equation of Equilibrium,

$$\frac{\partial\sigma_r}{\partial r} + \frac{\sigma_r - \sigma_\theta}{r} = 0 \quad \text{Eq. (15)}$$

Using the condition of rupture (Mohr circle) $(\sigma_r - \sigma_\theta) = (\sigma_r + \sigma_\theta)\sin\phi + 2C.\cos\phi$ Eq. (16)

Thus, $\frac{\sigma_\theta + C.\cot\phi}{\sigma_r + C.\cot\phi} = \frac{1-\sin\phi}{1+\sin\phi}$ Eq. (17)

Change of volume of the cavity = change of volume of the elastic zone + change of volume of the plastic zone + change of volume of SCP

Change of volume of the cavity = $R^2_u - R^2_i$

Change of volume (decrease) of the elastic zone = $(R^2_s - R^2_p) - \{(R_s + u_s)^2 - (R_p + u_p)^2\}$

Change of volume of the plastic zone = $(R^2_p - R^2_u)\Delta$

Change of volume of SCP = $(R_s + u_s)^2 - R^2_s$

$R^2_u - R^2_i = [(R^2_s - R^2_p) - \{(R_s + u_s)^2 - (R_p + u_p)^2\}] + [(R^2_p - R^2_u)\Delta] + [(R_s + u_s)^2 - R^2_s]$

Neglecting higher order terms of u_p and u_s and assuming $R_i = 0$,

$1 + \Delta = \frac{2R_p}{R^2_u}u_p + \frac{R^2_p}{R^2_u}\Delta$ then $[\frac{R_u}{R_p}]^2(1+\Delta) = \frac{2u_p}{R_p} + \Delta$ therefore, $\{[\frac{R_u}{R_p}]\ (1+\Delta)^{\frac{1}{2}}\}^2 = \frac{2u_p}{R_p} + \Delta$

but $(1+\Delta)^{\frac{1}{2}} \approx 1$ so $[\frac{R_u}{R_p}]^2 = \frac{2u_p}{R_p} + \Delta$ Eq. (18)

as $u_p = \frac{(1+\upsilon)R_p}{(R_s^{\ 2} - R_p^{\ 2})E}[(1-2\upsilon)\{(\sigma_p - q)R_p^{\ 2} - u_s k_h R_s^{\ 2}\} + (\sigma_p - q - u_s k_h)R_s^{\ 2}]$ Eq. (19)

Proof of Eq. (19):

Solution for equation (15) (after Timoshenko & Goodier 1951)

$\sigma_r = \frac{A}{r^2} + A_1$

$$\sigma_\theta = \frac{A}{r^2} + A_1$$

when $(\sigma_r)_{r=R_p} = (\sigma_p - q) and (\sigma_r)_{r=R_s} = u_s k_h$:

$$A = \frac{R_s^{\,2} R_p^{\,2} (\sigma_p - q - u_s k_h)}{(R_s^{\,2} - R_p^{\,2})} \quad 2A_1 = -\frac{R_s^2 \left(\sigma_p - q\right) - u_s k_h R_s^2}{\left(R_s^2 - R_p^2\right)}$$

For elastic materials.

$$\varepsilon_r = -\frac{du}{dr} \text{ and } \varepsilon_\theta = -\frac{u}{r} \qquad \varepsilon_r = \frac{d(r\varepsilon_\theta)}{dr} \qquad \varepsilon_r = \frac{1-\upsilon^2}{E}[\sigma_r - \frac{\upsilon}{1-\upsilon}\sigma_\theta]$$

$$\varepsilon_\theta = \frac{1-\upsilon^2}{E}[\frac{-\upsilon}{1-\upsilon}\sigma_r + \sigma_\theta] \qquad u = -r.\varepsilon_\theta$$

$$u = -\frac{r(1-\upsilon^2)}{E}\{-\frac{\upsilon}{1-\upsilon}[2C + \frac{A}{r^2}] + [2C - \frac{A}{r^2}]\}$$

$$u = -\frac{r(1+\upsilon)}{E}\{2C(1-2\upsilon) - \frac{A}{r^2}\}$$

$$u = \frac{r(1+\upsilon)}{E}\{[(1-2\upsilon)\frac{R_p^{\,2}(\sigma_p - q) - u_s k_h R_s^{\,2}}{(R_s^{\,2} - R_p^{\,2})}] + \frac{1}{r^2}\frac{R_s^{\,2} R_p^{\,2}(\sigma_p - q - u_s k_h)}{(R_s^{\,2} - R_p^{\,2})}]\}$$

when $r = R_p$ and $u = u_p$ then,

$$u_p = \frac{R_p(1+\upsilon)}{(R_s^{\,2} - R_p^{\,2})E}[(1-2\upsilon)\{(\sigma_p - q)R_p^{\,2} - u_s k_h R_s^{\,2}\} + (\sigma_p - q - u_s k_h)R_s^{\,2}]$$

and when $r = R_s$ and $u = u_s$ then,

$$u_s = \frac{R_s(1+\upsilon)}{(R_s^{\,2} - R_p^{\,2})E}[(1-2\upsilon)\{(\sigma_p - q)R_p^{\,2} - u_s k_h R_s^{\,2}\} + (\sigma_p - q - u_s k_h)R_p^{\,2}] \qquad \text{Eq. (20)}$$

Therefore from (Eq. (18) and Eq. (19),

$$[\frac{R_u}{R_p}]^2 = \frac{2(1+\upsilon)}{(R_s^{\,2} - R_p^{\,2})E}[(1-2\upsilon)\{(\sigma_p - q)R_p^{\,2} - u_s k_h R_s^{\,2}\} + (\sigma_p - q - u_s k_h)R_s^{\,2}] + \Delta \qquad \text{Eq. (21)}$$

and then the solution becomes,

$$\sigma_r = \frac{R_s^{\,2} R_p^{\,2}(\sigma_p - q - u_s k_h)}{(R_s^{\,2} - R_p^{\,2})}\frac{1}{r^2} - \frac{R_p^{\,2}(\sigma_p - q) - u_s k_h R_s^{\,2}}{(R_s^{\,2} - R_p^{\,2})} \qquad \text{Eq. (22)}$$

$$\sigma_\theta = -\frac{R_s^{\,2} R_p^{\,2}(\sigma_p - q - u_s k_h)}{(R_s^{\,2} - R_p^{\,2})}\frac{1}{r^2} - \frac{R_p^{\,2}(\sigma_p - q) - u_s k_h R_s^{\,2}}{(R_s^{\,2} - R_p^{\,2})} \qquad \text{Eq. (23)}$$

Considering the compatibility condition at elastic-plastic boundary ;

$$\frac{\sigma_r + \sigma_\theta}{2} = q - \frac{R_p^{\,2}(\sigma_p - q) - u_s k_h R_s^{\,2}}{(R_s^{\,2} - R_p^{\,2})} \qquad \text{Eq. (24)}$$

$$(\sigma_r - \sigma_\theta) = (\sigma_r + \sigma_\theta)\sin\phi + 2c.\cos\phi$$

then, $\sigma_\theta = \frac{\sigma_r(1-\sin\phi) - 2C\cos\phi}{1+\sin\phi}$

so, $$\frac{\sigma_r+\sigma_\theta}{2}=\frac{\sigma_r+\frac{\sigma_r(1-\sin\phi)-2C\cos\phi}{1+\sin\phi}}{2}$$

By solving above equation with Eq. (24),

$$q-\frac{R_p{}^2(\sigma_p-q)-u_s k_h R_s{}^2}{(R_s{}^2-R_p{}^2)}=\frac{\sigma_r-C\cos\phi}{1+\sin\phi}$$ and at the boundary $\sigma_r = \sigma_p$

$$\sigma_p(R_s^2-R_p^2)-C.\cos\phi((R_s^2-R_p^2))=[(R_s^2-R_p^2)q-(\sigma_p-q)R_p^2+U_s k_h R_s^2](1+\sin\phi) \quad \text{Eq. (25)}$$

$$u_s=\frac{(1+\upsilon)R_s}{(R_s{}^2-R_p{}^2)E}[(1-2\upsilon)\{(\sigma_p-q)R_p{}^2-u_s k_h R_s{}^2\}+(\sigma_p-q-u_s k_h)R_p{}^2]$$

$$u_s[1+\frac{(1+\upsilon)R_s}{(R_s{}^2-R_p{}^2)E}\{(1-2\upsilon)k_h R_s{}^2+k_h R_p{}^2\}=\frac{(1+\upsilon)R_s}{(R_s{}^2-R_p{}^2)E}[(1-2\upsilon)(\sigma_p-q)R_p{}^2+(\sigma_p-q)R_p{}^2]$$

$$\therefore u_s=\frac{2(1-\upsilon)(\sigma_p-q)R_p{}^2}{k_h\{(1-2\upsilon)R_s{}^2+R_p{}^2\}+\frac{E(R_s{}^2-R_p{}^2)}{(1+\upsilon)R_s}} \quad \text{Eq. (26)}$$

By using equations (16), (21), (22), (25) and (26) we can find that;

$$\sigma_p=\frac{C.\cos\phi(R_s{}^2-R_p{}^2)+R_s{}^2(1+\sin\phi)q-\frac{2(1-\upsilon)qR_p{}^2k_h}{k_h\{(1-2\upsilon)R_s{}^2+R_p{}^2\}+\frac{E(R_s{}^2-R_p{}^2)}{(1+\upsilon)R_s}}}{\{R_s{}^2+R_p{}^2\sin\phi-\frac{2(1-\upsilon)R_p{}^2k_h}{k_h\{(1-2\upsilon)R_s{}^2+R_p{}^2\}+\frac{E(R_s{}^2-R_p{}^2)}{(1+\upsilon)R_s}}\}} \quad \text{Eq. (27)}$$

For cylindrical case ultimate cavity pressure can be computed by using :

$$\sigma_p=\left(P_u+C\cot\phi\right)\left(\frac{R_u}{R_p}\right)^{\frac{2\sin\phi}{1+\sin\phi}}-C\cot\phi \quad \text{Eq. (28)}$$

For spherical case, ultimate cavity pressure can be computed by using :

$$\sigma_p=\left(P_u+C\cot\phi\right)\left(\frac{R_u}{R_p}\right)^{\frac{4\sin\phi}{1+\sin\phi}}-C\cot\phi \quad \text{Eq. (29)}$$

where P_u is the ultimate cavity pressure

5.0 Analysis Using Vesic Theory and Cavity Expansion Theory

The analysis was performed using Vesic theory and cavity expansion theory by varying the input parameters to suit the laboratory tests done under this research. MATLAB was used to solve the above-mentioned simultaneous equations and the most appropriate solution for a particular case was selected by avoiding negative and imaginary answers. The solutions contained multiple answers with only one suitable answer.

These theories simulate the behavior of the SCP with different internal friction angles and the behavior of the plastic zone and elastic zone within the SCP was observed by varying the radius of the SCP, coefficient of sub grade reaction, Modulus of elasticity and the radius of cone. A parametric study was done in order to find the relationship between the independent parameters and the dependent parameters of the above expressions.

5.1 Variables of the Parametric Study

The independent variables used for the analysis are as follows.

Angle of Internal Friction	- ϕ
Radius of the SCP	- R_s
Radius of the Cone	- R_c
Coefficient of the sub grade reaction	- K_h
Modulus of Elasticity	- E
Volumetric strain	- Δ

The dependent variables used for the analysis are as follows.

Radius of the plastic zone	- R_p
Stress in the plastic zone	- σ_p
Displacement at the SCP boundary	- U_s
Displacement at the plastic zone	-U_p

To simplify the analysis, Δ was used as an input parameter with a range of –0.01 to 0.02. Using the two outputs for R_p and σ_p, the ultimate cavity pressure (P_u) was calculated. A Poisson's ratio (υ) of 0.3 was used.

5.2 Parametric Study of Cone Penetration in Sand Using Cavity Expansion Theory

This section shows the behavior of several dependent parameters explained earlier based on cavity-expansion theory. The main objective of this is to obtain a relationship between ultimate cavity pressure and the drained friction angle. For this purpose, Toyoura sand properties, such as modulus of elasticity, Poisson's ratio and the coefficient of sub-grade reaction, were obtained from previously published papers. Two types of cases, such as cylindrical cavity and spherical cavity, were studied using cavity expansion theory and compared with Vesic solutions.

5.3 Ultimate Cavity Pressure versus Angle of Friction

Several non-dimensional relationships, which are directly related with ultimate cavity pressure and the angle of friction, are discussed in this section. The comparison of Pu/σ_c versus Friction Angle for Vesic and Cavity Expansion Theories for 2D and 3D are shown in the Figure 6 and Figure 7 respectively, and the same comparison of P_u/σ_c versus $\tan(\phi)$ for Vesic and Cavity Expansion Theories for 2D and 3D are shown in Figure 8 and Figure 9, respectively. It is quite clear that there is a considerable difference in values between 2D and 3D, although Vesic theory and Cavity expansion theory tally in both cases. The P_u value for the 2D case is much less than for the 3D case for the same friction angle. For both cases, the Vesic results and the cavity expansion results for infinite soil mass are almost the same and it is exactly the same for the 2D case even though two approaches were followed to achieve this result.

5.4 Normalized Ultimate Cavity Pressure versus Normalized Elastic Modulus

The Pu/σ_c versus E/σ_c relationship for 2D and 3D cases, are shown in Figure 10. For this parametric study, the E value was taken as the input parameter i.e. as the independent variable, and the variation in the ultimate cavity pressure was observed. The same result was obtained for all four cases of confining stresses for a particular SCP radius and volumetric strain. It was observed that for zero volumetric strain, the ultimate cavity pressure (Pu) is greater compared to other volumetric strains independent of whatever the confining stress used. The Pu value was very high for a low E for the 2D case in comparison to the 3D case. Also, for a higher SCP radius, the Pu value is greater compared to a low SCP radius like 2.5 cm.

5.5 Normalized Ultimate Cavity Pressure versus Volumetric Strain (Pu/σ_c versus Δ)

Pu/σ_c versus Δ relationships for 2D and 3D cases are shown in Figure 11 and Figure 12. A similar relationship is observed for both the 2D and 3D cases. According to these two graphs, higher R_s/R_{cone} (i.e. higher SCP radius) generates the highest Pu value compared to low R_s/R_{cone} cases. For the laboratory tests, R_s/R_{cone} = 8.33 was used, and this value is much less than the actual value. It should be noted that Pu/σ_c for a smaller R_s/R_{cone} is very small compared to a high R_s/R_{cone}.

5.6 Radial Displacement (U_r) versus the Radius (r) from the Center of the Cone

By considering all the cases of volumetric strains for 2D and 3D, it can be observed (Figure 13) that the radial displacement (Ur) will approach towards a very small constant level of 0.001 cm from a comparatively higher level of 0.1cm.

5.7 Normalized Ultimate Cavity Pressure versus R_s/R_{cone}

Pu/σ_c versus R_s/R_{cone} relationships are shown in Figure 14, Figure 15 and Figure 16 for negative volumetric strain, zero volumetric strain and positive volumetric strain respectively. It can be seen that there is a good agreement for all of these cases above for low values of R_s/R_{cone} (i.e. up to 10). There is a large difference for the positive case, which is shown in Figure 16, where the, values of Pu/σ_c are much less than the negative volumetric strain and zero volumetric strain cases. The variation due to the different confining stresses, for this case, is also very small compared to the other two cases. Figure 17 shows the same variation for the zero volumetric strain case for 2D. When this is compared with Figure 15, which shows the variation for the 3D case, the 3D condition shows a higher Pu/σ_c than the 2D case.

5.8 Normalized Ultimate Cavity Pressure versus Normalized Coefficient of Sub-grade Reaction

Figure 18 shows the relationship between Pu/σ_c versus k/σ_c for the 3D case. According to this figure, high confining stresses have a low Pu value for the same coefficient of sub-grade reaction. The variation of Pu/σ_c is small, and it is from 18.35 to 19.35. This means that Pu/σ_c variation with k/σ_c is negligible.

5.9 Displacement versus Angle of Friction

The variation of displacement at the SCP boundary (U_s) with tan (ϕ) is shown in Figure 19, and this shows that low confining stresses have lower displacements compared to high confining stresses when a cone is penetrated. U_s and U_p (displacement at the plastic boundary) variation with the plastic zone radius is shown in Figure 20, and it appears that there is a high tendency of having high displacements at a low R_p for high confining stresses.

5.10 Normalized Ultimate Cavity Pressure versus Volumetric Strain

Pu/σ_c versus volumetric strain relationship for Vesic theory is shown in Figure 21. According to these results, there is low Pu/σ_c value for high confining stresses with negative volumetric strain.

5.11 Practical Aspects of this Study

Analytical approach presented in this study can provide a means to evaluate the mechanical properties of SCP by using CPT. This study suggested that cavity expansion approach provide a more accurate prediction of cone resistance than bearing capacity theory, because the influence of soil stiffness and compressibility can all be adequately taken into account.

6.0 Conclusions

6.1 Cavity Expansion Theory and Vesic Equations

The following conclusions can be made by comparing the final results of cavity expansion theory with the results from Vesic equations for an infinite soil mass.

1. When cavity expansion theory for 2D was compared with the Vesic equation results, it was observed that the results were exactly the same and it can be concluded that the derivation exactly matches for infinite condition.

2. Similarly, when the results for the 3D cases were compared, it was observed that the results were almost the same, with little difference as the confining stresses increase.

6.2 Parametric Study Using Cavity Expansion Theory

The following conclusions can be made based on the parametric study done using the developed theory.

1. Ultimate cavity pressure (normalized with confining stress) variation with modulus of elasticity (normalized with confining stress) clearly showed the same result for all four confining stresses used here for a particular volumetric strain, radii of cone and SCP. The results varied depending on the type of analysis (2D or 3D).

2. 2D analyses gave lower values for ultimate cavity pressure than 3D analysis in the above-mentioned variation. This also shows the same result of giving high ultimate cavity pressure values for 3D case as observed in the other variations.

3. Ultimate cavity pressure was higher for lower volumetric strains when compared with higher volumetric strains. For negative volumetric strains, ultimate cavity pressure is more than for positive values. This means, the expansion of volume due to penetration of a cone will lead to higher stresses than contraction.

4. Ultimate cavity pressure (normalized with confining stress) variation with R_{SCP}/R_{cone} for different confining stresses yielded almost the same result with a very small difference. When this result is compared with the practically available ratios of R_{SCP}/R_{cone}, it can be concluded that when the R_{SCP}/R_{cone} is greater than 20, the ultimate cone penetration value is a constant.

5. Higher confining stresses give higher displacements at the SCP boundary depending on the volumetric strain, elastic modulus and the coefficient of sub-grade reaction.

7.0 Acknowledgement

The author expresses his thanks to the ASIAN INSTITUTE OF TECHNOLOGY for giving facilities for this study during his Masters studies at AIT and gratefully acknowledges the kind help given by his advisor, Dr.Jiro Takemura during this study.

8.0 References

1. Chen, J.W., and Juang, C.H. (1996), "Determination of Drained Friction Angle of Sands from CPT", Journal of Geotechnical Engineering, Vol. 122, No. 5, pp374-381.

2. Dunham, J.W. (1954). "Pile Foundations for Buildings", ASCE Journal of Soil Mechanics and Foundation Division, pp385-1 385-21

3. Salgado, R., Mitchell, J.K., and Jamiolkowski, M. (1997)."Cavity Expansion and Penetration Resistance in Sand". Journal of Geotechnical and Geoenvironmental Engineering, pp344-354

4. Soil Mechanics Group (2001), " Report of Contract Research on Stability of Caisson Type Quay Wall of Clay Improved by SCP", Tokyo Institute of Technology (In Japanese)

5. Timoshenko, S., and Goodier, J.N. (1951). "Theory of Elasticity", Two Dimensional Problems in Polar Coordinates, McGraw-Hill, pp58-62

6. Vesic, A.S. (1972). "Expansion of Cavities in Infinite Soil Mass". Journal of the Soil Mechanics and Foundations Division, ASCE, SM3, pp265-290.

7. Yu, H. (2000). "Cavity Expansion Methods in Geomechanics", Kluwer Academic Publishers, pp09-24, London.

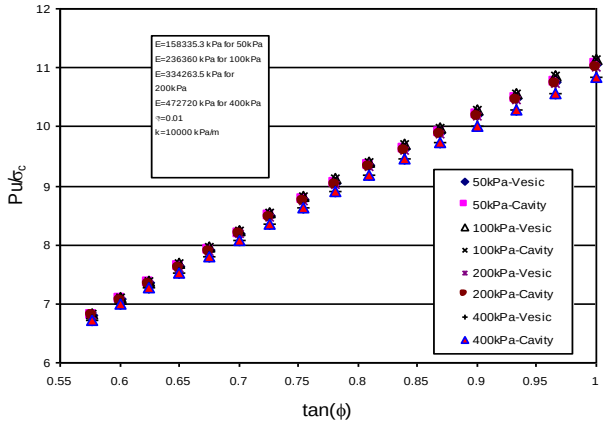

Figure 6. Normalized Ultimate Cavity Pressure versus Friction Angle for 2D Case

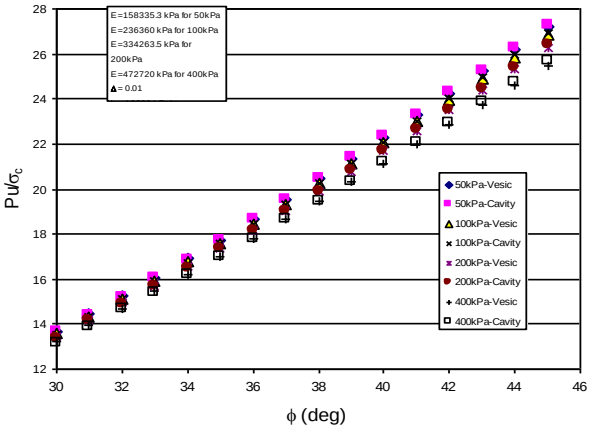

Figure 7. Normalized Ultimate Cavity Pressure versus Friction Angle for 3D Case

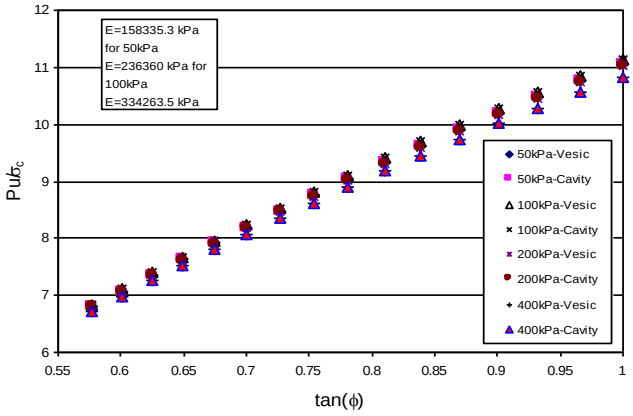

Figure 8. Normalized Ultimate Cavity Pressure versus tan ϕ for 2D Case

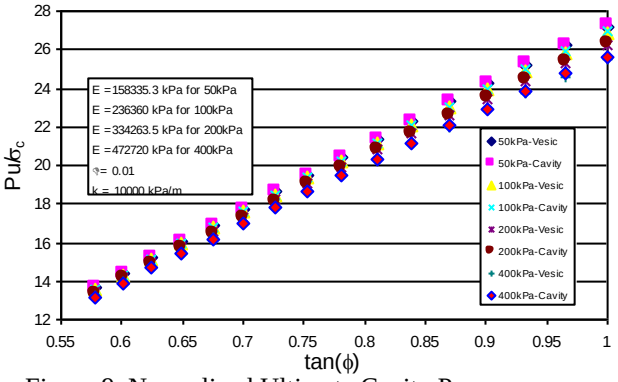

Figure 9. Normalized Ultimate Cavity Pressure versus tan ϕ for 3D Case

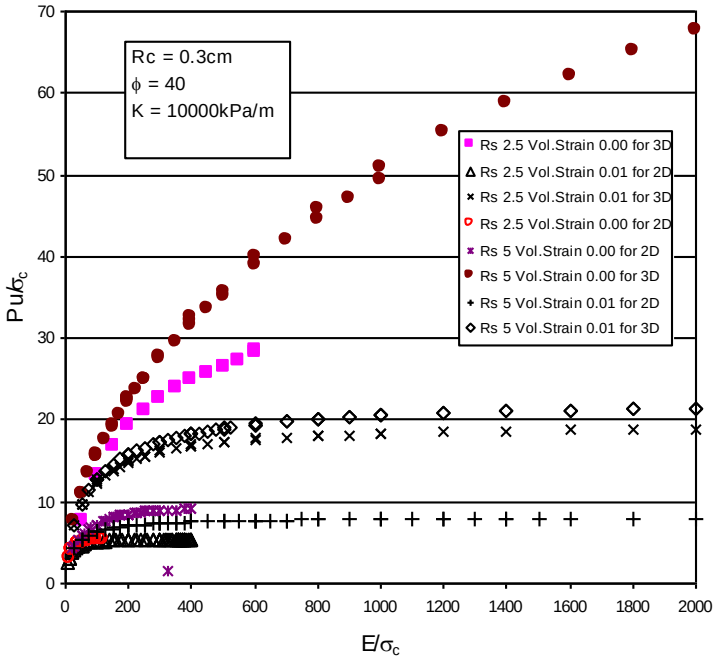

Figure 10. Normalized Ultimate Cavity Pressure versus Normalized Elastic Modulus

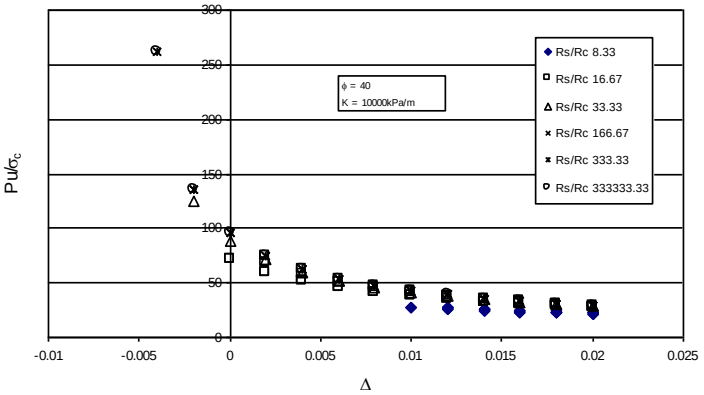

Figure 11. Normalized Ultimate Cavity Pressure versus Volumetric Strain for 2D Case

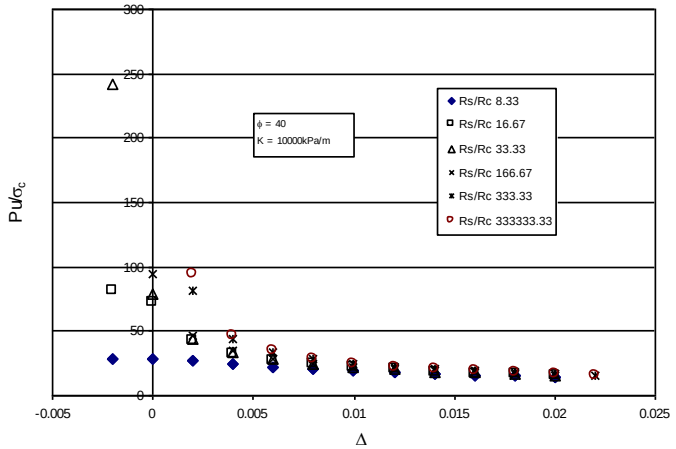

Figure 12. Normalized Ultimate Cavity Pressure versus Volumetric Strain for 3D Case

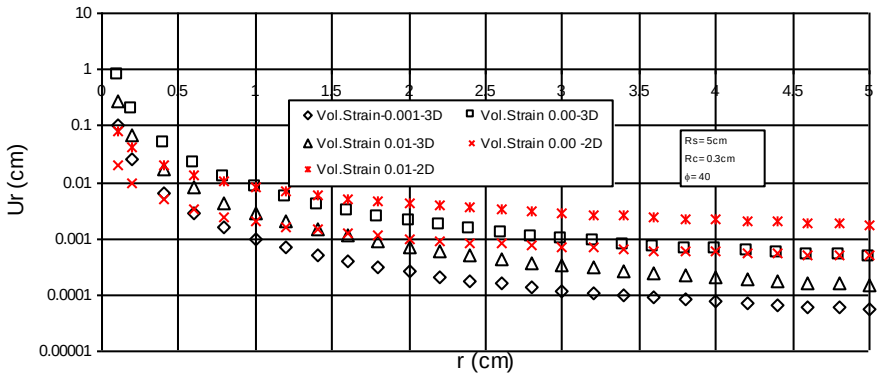

Figure 13. Radial Displacement versus Radius from the Center of the Cone

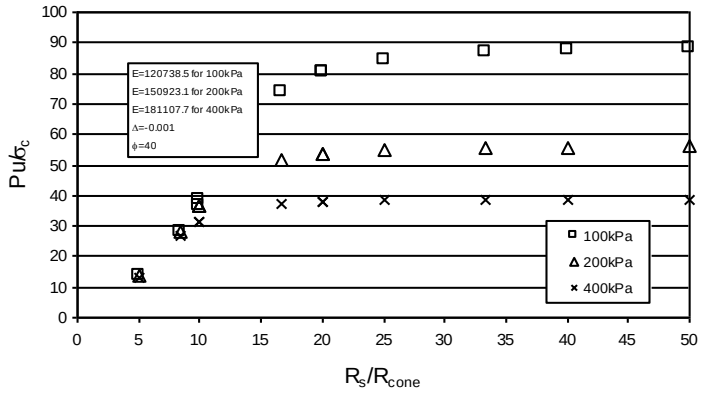

Figure 14. Normalized Ultimate Cavity Pressure versus R_s/R_{cone} for Negative Volumetric Strain

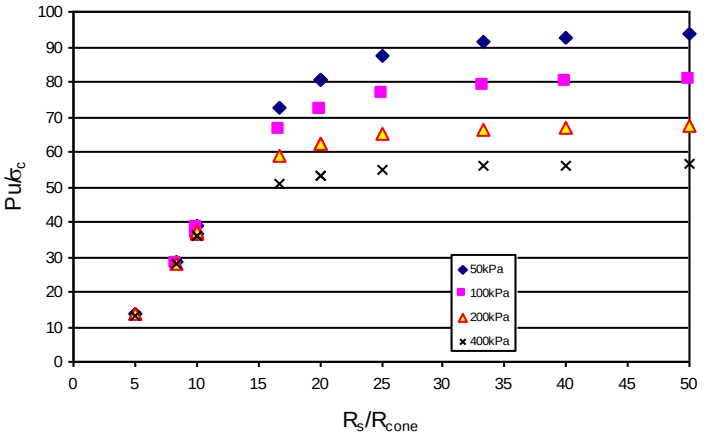

Figure 15. Normalized Ultimate Cavity Pressure versus R_s/R_{cone} for Zero Volumetric Strain

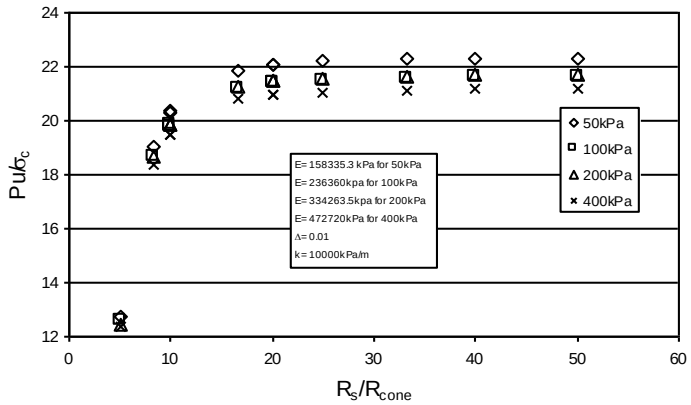

Figure 16. Normalized Ultimate Cavity Pressure versus R_s/R_{cone} for Positive Volumetric Strain

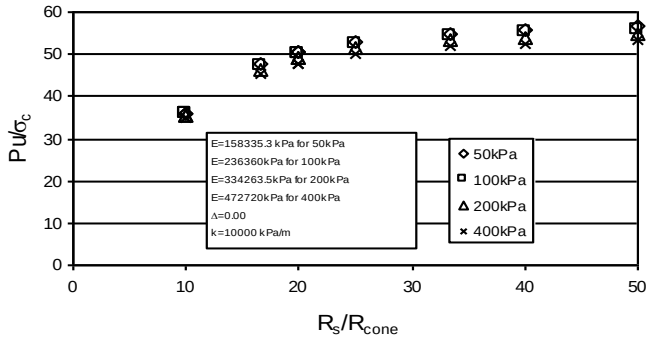

Figure 17. Normalized Ultimate Cavity Pressure versus R_s/R_{cone} for Zero Volumetric Strain – 2D

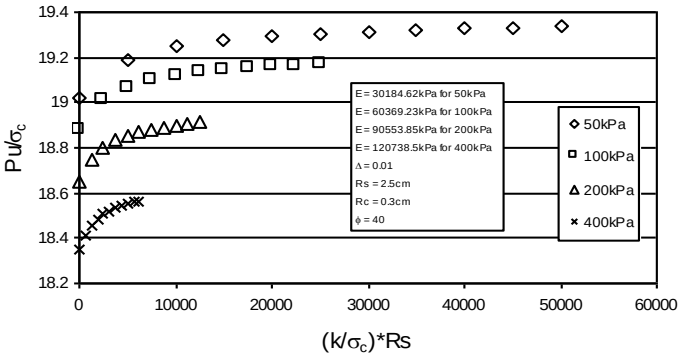

Figure 18. Normalized Ultimate Cavity Pressure versus Normalized Coefficient of Sub-grade Reaction

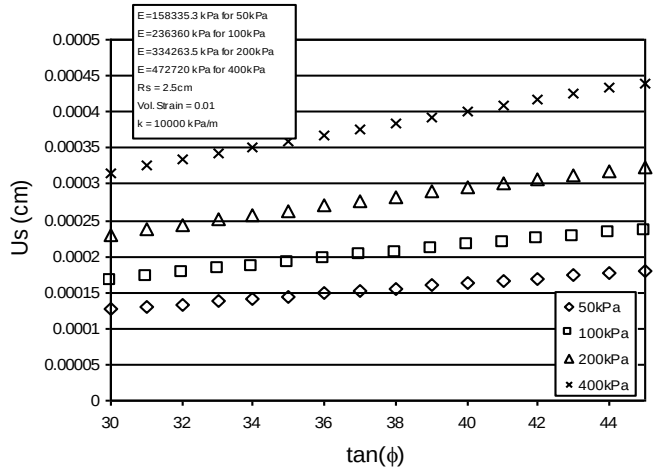

Figure 19. Displacement at the SCP Boundary versus tan (ϕ)

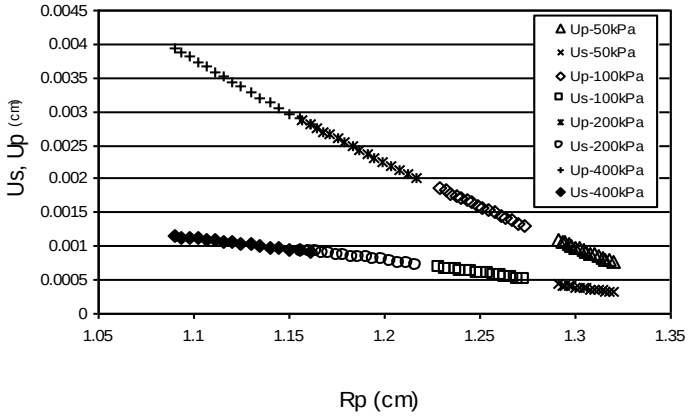

Figure 20. Displacement at the SCP Boundary and the Plastic Boundary versus Plastic Zone Radius

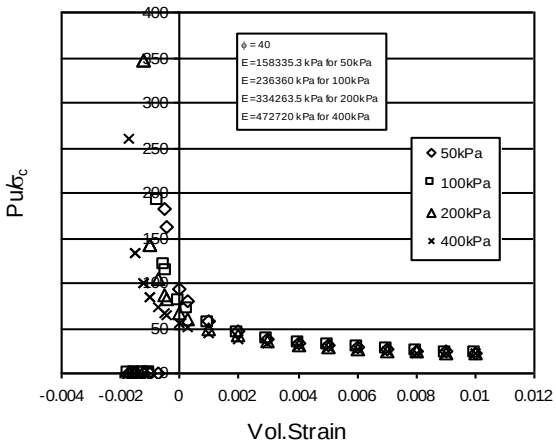

Figure 21. Normalized Ultimate Cavity Pressure versus Volumetric Strain – Vesic Theory